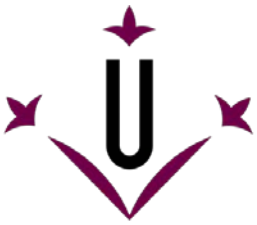

Radiative cooling as low-grade energy source: A literature review

Sergi Vall, Albert Castell

Department of Computer Science and Industrial Engineering, University of Lleida, Edifici CREA, Pere de Cabrera s/n, 25001 Lleida, Spain

Abstract

Radiative cooling is a technology intended to provide cooling using the sky as a heat sink. This technology has been widely studied since 20th century but its research is scattered all over the literature, requiring of a review to gather all information and a state-of-the-art. In the present article, the research has been classified in: (1) radiative cooling background, (2) selective radiative cooling, (3) theoretical approach and numerical simulations, and (4) radiative cooling prototypes. Even though this is a low-grade technology it can dramatically reduce the energy consumption, since it is renewable and requires low energy for its operation. However, new functionalities of the device, apart from radiative cooling, are required for profitable reasons. Some recommendations extracted from the literature to improve the efficiency of radiative cooling are: to use a cover to achieve low temperatures, to use water instead of air as heat-carrier fluid, and to couple the device with heat storage. Finally, further research should be focused in the development of new materials with improved radiative properties, the measurement of incoming infrared atmospheric radiation and/or new technics to predict it, and the evaluation of new device concepts.

Keywords

Radiative cooling, Renewable cooling, Night sky radiation, Low-grade cooling.

1. Introduction

The environmental awareness is growing fast nowadays with special attention to the energy consumption and environment preservation. Regarding to energy consumption, the building sector can contribute in a remarkable way in achieving the transition to a less energy intensive system. There is huge potential in reducing energy consumption with profitable measures that reduce the economic and environmental costs. The energy consumption of buildings represents 40% of total energy consumption in the European Union [1], where space conditioning of buildings represents almost half of the building energy consumption.

For space conditioning, especially in hot climate countries, most of the buildings use reversible heat pumps which consume a large amount of electrical energy. New legislations consider

electrically driven heat pumps as a renewable source of energy when they achieve seasonal average efficiencies higher than $SCOP_{NET} \geq 2.5$ [2,3], since they take advantage of the air temperature to reduce electrical consumption. However, there are other renewable sources that further reduce the use of non-renewable energy, since they can achieve the required temperature level with no or very low electrical use. Solar energy is one of the most widely studied sources; however, its use for cooling is limited by the implementation of absorption heat pumps.

Another technology that has been studied in order to provide cooling and displace the use of heat pumps is radiative cooling. This technique is based on emitting long-wave thermal radiation from a terrestrial body toward space through the infrared atmospheric window between 8-13 μm wavelengths. The atmosphere infrared window is the dynamic behaviour of earth's atmosphere that allows some infrared radiation pass through the atmosphere without being absorbed and, thus without heating the atmosphere.

It is known that a body emits electromagnetic radiation in a wavelength range depending on its temperature. At ambient temperature most of the radiation is emitted in the infrared spectrum. Radiative cooling technique uses these properties to generate a cooling net balance between the emitted thermal radiation from the terrestrial surface and the received from the atmosphere.

Using this technology for cooling purposes will dramatically reduce the energy consumption; depending on the case, the energy consumption can be zero or just the energy consumed by a small pump running on the operating hours. The performance of the radiative cooling technology is affected by the physical properties of the device and also by the surrounding conditions. Therefore, special attention must be paid to materials and environmental conditions.

From early 20th century, several authors have worked on the field of radiative cooling. However, in the present all the information is scattered in the literature, making it difficult to identify new research opportunities. Although Lu et al. developed a practical review of radiative cooling [4], they focused in passive radiative cooling in buildings, and they did not include detailed information about the phenomenon and the studied materials for radiative cooling as well as the radiative cooling devices and models. Therefore, there is a clear need to compile and structure all this information. For that reason, this paper reviews all different aspects of radiative cooling, such as the environmental conditions affecting the phenomena, the selection and development of materials, the analytical and numerical methods, and the experimental prototypes.

2. Radiative cooling background

Radiative cooling is the thermal process by which a body loses heat by emitting long-wave radiation to another body at lower temperature. Referred to buildings, radiative cooling is a

passive cooling technique which uses thermal radiation properties to cool a body or part of a building facing a colder surface such as the sky. This cooling process occurs when a surface presents a cooling net balance between the emitted and the absorbed radiation, considering also convection and conduction between the surface and the surroundings. With this technique, temperatures below ambient temperature can be achieved. The effective outgoing infrared radiation from a surface on earth (R) is defined as the difference between the infrared radiation emitted by this surface $(R_{\uparrow})$ and the infrared radiation from the atmosphere absorbed by this surface $(R_{\downarrow})$ (Eq. 1) [5]:

$$R = R_{\uparrow} - R_{\downarrow} \qquad \text{Eq. 1}$$

The spectral distribution of the radiation emitted by the clear sky atmosphere is similar to a blackbody's one at ambient dry bulb temperature but with a gap in the spectral region between wavelengths 8-13 μm. This gap is known as "infrared atmospheric window".

Research has been conducted in order to determine and analyse the infrared atmospheric window while analysing the atmospheric infrared radiation [6]. The spectral location of the infrared atmospheric window corresponds to the spectrum where most of the terrestrial surfaces emit with its maximum intensity.

2.1. Infrared atmospheric radiation

Atmospheric radiation originates from gases that compose the atmosphere such as water vapour, carbon dioxide, ozone, and other asymmetrical molecules. 90 percent of the total infrared atmospheric radiation received at ground level comes from the first 800-1600 meters above the surface [5]. The main gases involved in infrared atmospheric radiation at ground level are water vapour and carbon dioxide, being water vapour the major contributor [7]. Analysing the radiative properties of these gases can be seen that the atmosphere spectrum in the 8-13 μm band (infrared atmospheric window) is very transparent under clear sky conditions [8].

These dynamic properties of earth's atmosphere make the atmosphere an interesting heat sink to eliminate heat excess. As the atmosphere does not act like a blackbody emitter, it is difficult to predict its behaviour although the physical phenomenon can be physically described as it was presented in [4]. Therefore, for engineering purposes, it would be interesting to measure and/or predict the incoming infrared radiation from the atmosphere on a surface facing the sky.

This data can be measured with specific equipment or predicted with some empirical correlations. When the incoming infrared radiation from the atmosphere is known, there are two methods to express it in an understandable and simple form:

1. To assume the sky acting as a blackbody emitter (effective sky emissivity $\varepsilon_{sky} = 1$) at an effective sky temperature (T_{sky}) which equals the incoming infrared radiation from the atmosphere based on the Stefan-Boltzmann law (Eq. 2):

$$\text{Eq. 2} \qquad R_{\downarrow} = \sigma \cdot T_{sky}^4 \rightarrow T_{sky} = \left(\frac{R_{\downarrow}}{\sigma}\right)^{1/4}$$

2. To assume the sky having the ambient dry bulb temperature (T_a) with an effective sky emissivity (ε_{sky}) which equals the radiation coming from the atmosphere based on the Stefan-Boltzmann law (Eq. 3):

$$\text{Eq. 3} \qquad R_{\downarrow} = \varepsilon_{sky} \cdot \sigma \cdot T_a^4 \rightarrow \varepsilon_{sky} = \frac{R_{\downarrow}}{\sigma \cdot T_a^4}$$

These two methods simplify the way the incoming infrared radiation from the atmosphere is quantified for engineering calculations. However, the incoming infrared atmospheric radiation is not commonly measured in meteorological stations; therefore, correlations must be elaborated to connect measured simple meteorological parameters to the infrared atmospheric radiation.

There are two types of methods to estimate the incoming infrared radiation from atmosphere under clear sky conditions [8]. The first type is based on direct measurements of the atmosphere radiation spectrum or sky irradiance. These empirical methods use measurements of the incoming infrared atmospheric radiation to generated suitable correlations. The second type consists on analysing the profiles of atmospheric constituents to calculate their spectral atmospheric radiation based on radiative properties of the gases. Although more rigorous, this second type is more complex, and detailed information on the state of the atmosphere is needed, such as pressure, temperature and density variation with altitude, concentration profiles and spectral absorption coefficients of the gases.

2.1.1. Clear sky correlations

Making a proper estimation of the incoming infrared atmospheric radiation is important for modelling and engineering purposes. Although estimations never adapt perfectly to the reality, neither clear sky is the most common condition depending on the weather; however they can be enough accurate as a first approach. In this section, different correlations for clear sky conditions are presented and reviewed, distinguishing between empirical and detailed correlations.

Empirical correlations

Empirical correlations are based on total atmospheric radiation measurements made with a pyrgeometer. A pyrgeometer is a device that measures downward atmospheric long wave radiation. In some measurements a spectral radiometer was also used to calibrate the pyrgeometer and also to detect the presence of clouds.

However, these measurements do not provide any spectral information of the incoming infrared atmospheric radiation. This is a simple way to estimate the incoming infrared atmospheric radiation but it cannot be enough accurate for some calculations, especially when spectral information is required.

First works providing a correlation were presented by Ångström (1915 and 1936) [9,10] and Brunt (1832) [11], relating sky emissivity to the partial pressure of water vapour (Eq. 4 and Eq. 5). Both correlations are based in clear-sky atmospheric radiation values measured in specific locations (Algeria and California).

$$\text{Eq. 4} \qquad \varepsilon_{sky,0} = \alpha - \beta \cdot 10^{-\gamma \cdot e_0} \rightarrow (\text{Ångström}) \tag{4}$$

$$\text{Eq. 5} \qquad \varepsilon_{sky,0} = a + b \cdot \sqrt{e_0} \rightarrow (Brunt) \tag{5}$$

These expressions require the calculation of some empirical coefficients $(a, b, \alpha, \beta, \gamma)$ which are somewhat variable and depend on the geographical region. Later works calculated empirical coefficients for Ångström's and Brunt's equations considering different meteorological and geographical conditions. A compilation of theses coefficients can be found in Elsasser [12] and Kondratyev [13], where significant discrepancies can be seen in the coefficients found for different locations.

Later on, Elsasser (1942) concluded that the sky emissivity has a logarithmic relation with the partial pressure of water vapour [12], developing a new correlation (Eq. 6).

$$\text{Eq. 6} \qquad \varepsilon_{sky,0} = 0.21 + 0.22 \cdot \ln(e_0) \tag{6}$$

While the previous correlations to estimate the incoming infrared atmospheric radiation depend on the partial pressure of water vapour, later works use ambient temperature as the main parameter.

Swinbank (1963) [14] conducted a reassessment of previous work published in [9–11] on the attempt to avoid local specificity of the correlation coefficients (as demonstrated in [12]) and proposed alternatively a correlation that only depends on ambient temperature, showing the low influence of humidity at low level stations (Eq. 7).

Eq. 7 $$R_{\downarrow,0} = 5.31 \cdot 10^{-14} \cdot T_a^6 \rightarrow \varepsilon_{sky,0} = 9.35 \cdot 10^{-6} \cdot T_a^2$$

From original equation it is readapted to have it in function of $\varepsilon_{sky,0}$.

Swinbank's correlation [14] attempted to be general. However, Idso and Jackson (1969) [15] stated that, based on new findings, Swinbank's correlations were not general. Therefore, they attempted to relate atmospheric radiation to ambient temperature to a universally applicable correlation which should be valid for any air temperature reached on earth and for any latitude (Eq. 8). However, in a following work [16], Aase and Idso concluded that below 273 K this correlation overestimates the total effective emissivity.

Eq. 8 $$\varepsilon_{sky,0} = 1 - \left(0.261 \cdot e^{-7.77 \cdot 10^{-4} \cdot (273.15 - T_a)^2}\right)$$

In 1983, Hatfield et al. [17] concluded that correlations models which only use ambient temperature [14,15] do not estimate properly the effective emissivity over wide geographical areas. They concluded that these models are too specific for a location because they assume a relationship between ambient temperature and partial pressure of water vapour in their empirical constants. From here on, authors developed correlations which depend on both ambient temperature and partial pressure of water vapour.

Satterlund (1979) [18], based on experimental measurements from literature, proposed a new correlation to take into account both ambient temperature and vapour pressure (Eq. 9). This correlation presents improvements on estimating the incoming infrared atmospheric radiation over a wide range of temperatures, particularly at low temperatures where most of the formulas perform poorly for air temperatures below freezing. This model has also probed to perform better when compared to two other models [15,19] (see Detailed method section).

Eq. 9 $$\varepsilon_{sky,0} = 1.08 \cdot \left(1 - e^{e_0^{Ta/2016}}\right)$$

Idso (1981) [20] performed an experiment at Phoenix, Arizona (USA) to obtain measurements of the total incoming infrared atmospheric radiation and proposed two correlations for different wavelengths (10.5-12.5 μm in Eq. 10 and 8-13 μm in Eq. 11) and another one for the whole range (Eq. 12). The three correlations depend on the temperature and the partial pressure of water vapour.

Eq. 10 $$\varepsilon_{10.5-12.5,0} = 0.1 + 3.53 \cdot 10^{-8} \cdot e_0^2 \cdot e^{3000/T_a}$$

Eq. 11 $$\varepsilon_{8-13,0} = 0.24 + 2.98 \cdot 10^{-8} \cdot e_0^2 \cdot e^{3000/T_a}$$

Eq. 12 $$\varepsilon_{sky,0} = 0.7 + 5.95 \cdot 10^{-5} \cdot e_0 \cdot e^{1500/T_a}$$

Andreas and Ackley (1982) [21] proposed a modification of Eq. 12 to be used at the Arctic and the Antarctic where the concentration of aerosols in these remote areas is lower.

Eq. 13 $$\varepsilon_{sky,0} = 0.601 + 5.95 \cdot 10^{-5} \cdot e_0 \cdot e^{1500/T_a}$$

From here on, authors started to use other parameters such as altitude, dew point temperature, relative humidity, and ambient pressure in their correlations, trying to predict in a better way the incoming infrared atmospheric radiation.

Centeno (1982) [22] proposed a clear sky emissivity correlation based on measurements from the literature and his own measurements at Venezuela. This correlation takes into account the altitude, the ambient temperature and the relative humidity (Eq. 14). To develop this correlation the author forced the correlation to be constituted by the product of three functions, each dependant of a parameter.

Eq. 14 $$\varepsilon_{sky,0} = [5.7723 + 0.9555 \cdot 0.6017^{Z}] \cdot T_a^{1.893} \cdot H^{0.0665} \cdot 10^{-14}$$

Berdahl and Fromberg (1982) [8], based on their own measurements at three USA cities (Tucson, Arizona; Gaithersburg, Maryland; and St. Louis, Missouri), proposed two different correlations to estimate the sky emissivity: one for night-time (Eq. 15) and one for day-time (Eq. 16). These correlations only depend on the dew point temperature.

Eq. 15 $$\varepsilon_{sky,0} = 0.741 + 0.0062 \cdot T_{dp}\ (night)$$

Eq. 16 $$\varepsilon_{sky,0} = 0.727 + 0.0060 \cdot T_{dp}\ (day)$$

Later on, Berdahl and Martin (1984) [23] corrected a previous work [8] by using more measurements (also in USA: San Antonio, Texas; West Palm Beach, Florida; and Boulder City, Nevada) and proposed a new correlation (Eq. 17) with a diurnal correction factor (Eq. 18). Finally, Martin and Berdahl (1984) [24] further extended their correlation by adding a pressure correction factor (Eq. 19 and Eq. 20).

Eq. 17 $$\varepsilon_{sky,0} = 0.711 + 0.56 \cdot \left(\frac{T_{dp}}{100}\right) + 0.73 \cdot \left(\frac{T_{dp}}{100}\right)^2 + \Delta\varepsilon_h$$

Eq. 18 $$\Delta\varepsilon_h = 0.013 \cdot \cos\left(\frac{2\pi t}{24}\right)$$

Eq. 19 $$\varepsilon_{sky,0} = 0.711 + 0.56 \cdot \left(\frac{T_{dp}}{100}\right) + 0.73 \cdot \left(\frac{T_{dp}}{100}\right)^2 + \Delta\varepsilon_h + \Delta\varepsilon_e$$

Eq. 20 $$\Delta\varepsilon_e = 0.00012 \cdot (P_0 - 1000)$$

Berger et al. (1984) [25] based on measurements at Carpentras, France proposed a night-time correlation that depends on the dew point temperature (Eq. 21). Moreover, they also proposed a correlation for the whole day (Eq. 22), where the ambient temperature must be corrected (Eq. 23) in order to include annual and diurnal effects.

Eq. 21 $$\varepsilon_{sky,0} = 0.770 + 0.0038 \cdot T_{dp} \quad (night)$$

Eq. 22 $$\varepsilon_{sky,0} = 0.752 + 0.0048 \cdot T_{dp} \quad (all\ day)$$

Eq. 23 $$T_{a,corrected} = T_a + K(t) + L(t) \cdot (T_{dp} - T_a)$$

Alados-Arboledas and Jimenez (1988) [26] proposed a deviation correction factor (Eq. 24) to take into account the day-night and seasonal variation of the effective emissivity based on measurements in Granada, Spain. This correction factor was tested in Eq. 12 and Eq. 5, being Eq. 12 the one with better results.

Eq. 24 $$\Delta\varepsilon = A \cdot \sin\pi\left[\frac{t-t'}{\Delta t} - \left(\frac{f}{\Delta t}\right)\right] \quad t' + f \leq t \leq t' + \Delta t$$

The parameters in Eq. 24 should be calculated according to the region and the season.

Niemelä et al. (2001) [27], based on measurements at Sodankylä, Finland, proposed two correlations (Eq. 25 and Eq. 26) for cold and dry weather conditions which only depend on the partial water vapour pressure.

Eq. 25 $$(e_0 \geq 2) \rightarrow \varepsilon_{sky,0} = 0{,}72 + 0{,}009 \cdot (e_0 - 2)$$

Eq. 26 $$(e_0 < 2) \rightarrow \varepsilon_{sky,0} = 0.72 - 0.076 \cdot (e_0 - 2)$$

Tang et al. 2004 [28], based on measurements at Negev Highlands, Israel, proposed a correlation (Eq. 27) for warm and dry weather conditions which only depend on the dew point temperature.

Eq. 27 $$\varepsilon_{sky,0} = 0.754 + 0.0044 \cdot T_{dp}$$

Empirical correlations are designed to make estimations of the incoming infrared atmospheric radiation from the atmosphere in an easy way. A tendency to use the simplest atmospheric parameters that allow a proper estimation is observed. However, there is no agreement in which parameters are better. From the literature, the importance of the atmospheric humidity and the ambient temperature is demonstrated to provide a good regression. Nevertheless, using just one

or two parameters does not allow the correlation to be applicable at any location. Therefore, most of the correlations above are valid for specific locations and their empirical coefficients should be recalculated for new locations. Last tendencies are to provide correlations easy to use and location dependant.

It is also important to highlight that the difference in the correlations which use the same parameters is on the mathematical model that the authors choose to adapt the physical phenomena. Some of them are based on physical properties while others are based in a statistical approach.

Detailed method

Detailed methods are based on radiative properties of the gases that compound the atmosphere and on their concentration. They can provide a rigorous estimation of the incoming infrared atmospheric radiation, although they need detailed information. There are three methods: using the gas transmittance to estimate the atmospheric emissivity; using an accurate radiative-transfer models/modelization (LOWTRAN, MODTRAN, SBDART); and using a flux emissivity model.

Based on theoretical concepts of gas emissivity and empirical correlations for gas properties, Bliss (1961) [7] obtained sky emissivity values with the only dependence of dew point temperature (Eq. 28 created from data in [7]):

$$\text{Eq. 28} \qquad \varepsilon_{sky,0} = 0.8004 + 0.00396 \cdot T_{dp}$$

Staley and Jurica (1972) [29] proposed a correlation (Eq. 29) based on the analysis of the radiation properties of water vapour, carbon dioxide and ozone.

$$\text{Eq. 29} \qquad \varepsilon_{sky,0} = 0.67 \cdot e_0^{0,08}$$

Brutsaert (1975) [19], based on analytical correlations of atmosphere parameters, proposed a sky emissivity correlation (Eq. 30) which depends on the vapour pressure and the ambient temperature. Below 273 K this correlation underestimates the total effective emissivity [16].

$$\text{Eq. 30} \qquad \varepsilon_{sky,0} = 1.24 \cdot (e_0/T_a)^{1/7}$$

Prata (1996) [30], based on an emissivity model, proposed a correlation (Eq. 31) which depends on ambient temperature and partial pressure of water vapour. This model has been tested with experimental measurements from several locations and has also been assessed by using radiosonde profiles and an accurate radiative-transfer model (LOWTRAN-7) to find the coefficients. The model has also been compared to five previous models [14,15,18–20] showing a better performance.

Eq. 31 $$\varepsilon_{sky,0} = 1 - (1 - \xi) \cdot e^{-\sqrt{1.2+3\cdot\xi}} \quad \xi = 46.5 \cdot \left(\frac{e_0}{T_a}\right)$$

Dilley and O'Brien (1998) [31], based on parameterization of physical processes and using a computer software model (LOWTRAN), proposed two correlations (Eq. 32 and Eq. 33) which depend on ambient temperature and partial pressure of water vapour.

Eq. 32 $$\varepsilon_{sky,0} = 1 - e^{(-1{,}66\cdot\tau)} \quad \tau = 2.232 - 1.875\left(\frac{T_a}{273.15}\right) + 0.7356\sqrt{18.6\left(\frac{e_0}{T_a}\right)}$$

Eq. 33 $$\varepsilon_{sky,0} = \frac{1}{\sigma\cdot T_a^4} \cdot \left[59.38 + 113.7 \cdot \left(\frac{T_a}{273.15}\right)^6 + 96.96\sqrt{18.6\left(\frac{e_0}{T_a}\right)}\right]$$

The detailed method can provide good estimations of the incoming infrared atmospheric radiation. However, this method requires detailed information about atmosphere composition. It has been confirmed that radiative transfer modelling produces better results than previously published simple parameterizations based only on surface measurements [32].

There is a lack of comparisons between different correlations in the literature. There just exist few articles comparing correlations [18,30].

It is also important to highlight that measurements are sporadically made and not very regular in time and location. So this means that it is difficult to get available data that fits a specific climate.

Clear-sky correlations are a first approach, although they do not represent the common scenario. Moreover, most of the correlations do not provide real-time values but average values. Table 1 presents a summary of the correlations found in the literature for clear-sky conditions.

Table 1 Summary of clear-sky correlations.

Authors	Clear-sky correlations	Equation
Ångström (1915 and 1936) [9,10]	$\varepsilon_{sky,0} = \alpha - \beta \cdot 10^{-\gamma\cdot e_0}$	4
Brunt (1832) [11]	$\varepsilon_{sky,0} = a + b \cdot \sqrt{e_0}$	5
Elsasser (1942) [12]	$\varepsilon_{sky,0} = 0.21 + 0.22\ln(e_0)$	6
Bliss (1961) [7]	$\varepsilon_{sky,0} = 0.8004 + 0.00396T_{dp}$	28
Swinkbank (1963) [14]	$\varepsilon_{sky,0} = 9.35 \cdot 10^{-6} \cdot T_a^2$	7
Idso and Jackson (1969) [15]	$\varepsilon_{sky,0} = 1 - \left(0.261 \cdot e^{-7.77\cdot10^{-4}\cdot(273.15-T_a)^2}\right)$	8
Staley and Jurica	$\varepsilon_{sky,0} = 0.67 \cdot e_0^{0,08}$	29

(1972) [29]		
Brutsaert (1975) [19]	$\varepsilon_{sky,0} = 1.24 \cdot (e_0/T_a)^{1/7}$	30
Satterlund (1979) [18]	$\varepsilon_{sky,0} = 1.08 \cdot \left(1 - e^{e_0^{T_a/2016}}\right)$	9
Idso (1981) [20]	$\varepsilon_{sky,0} = 0.7 + 5.95 \cdot 10^{-5} \cdot e_0 \cdot e^{(1500/T_a)}$	12
Andreas and Ackley (1982) [21]	$\varepsilon_{sky,0} = 0.601 + 5.95 \cdot 10^{-5} \cdot e_0 \cdot e^{1500/T_a}$	13
Centeno (1982) [22]	$\varepsilon_{sky,0} = [5.7723 + 0.9555 \cdot (0.6017)^z] \cdot T_a^{1.893} \cdot H^{0.0665} \cdot 10^{-14}$	14
Berdahl and Fromberg (1982) [8]	$\varepsilon_{sky,0} = 0.741 + 0.0062T_{dp}\ (night)$ $\varepsilon_{sky,0} = 0.727 + 0.0060T_{dp}\ (day)$	15, 16
Berdahl and Martin (1984) [23]	$\varepsilon_{sky,0} = 0.711 + 0.56\left(\frac{T_{dp}}{100}\right) + 0.73\left(\frac{T_{dp}}{100}\right)^2 + \Delta\varepsilon_h$ $\Delta\varepsilon_h = 0.013\cos\left(\frac{2\pi t}{24}\right)$	17, 18
Martin and Berdahl (1984) [24]	$\varepsilon_{sky,0} = 0.711 + 0.56\left(\frac{T_{dp}}{100}\right) + 0.73\left(\frac{T_{dp}}{100}\right)^2 + \Delta\varepsilon_h + \Delta\varepsilon_e$ $\Delta\varepsilon_e = 0.00012(P_0 - 1000)$	19, 20
Berger et al. 1984 [25]	$\varepsilon_{sky,0} = 0.770 + 0.0038 \cdot T_{dp} \quad (night)$ $\varepsilon_{sky,0} = 0.752 + 0.0048 \cdot T_{dp} \quad (all\ day)$	21, 22
Alados-Arboledas and Jimenez (1988) [26]	$\Delta\varepsilon = A\sin\pi\left[\frac{(t-t')}{\Delta t} - \left(\frac{f}{\Delta t}\right)\right]$	24
Prata (1996) [30]	$\varepsilon_{sky,0} = 1 - (1+\xi)\cdot e^{-\sqrt{1.2+3\cdot\xi}} \quad \xi = 46.5\cdot\left(\frac{e_0}{T_a}\right)$	31
Dilley and O'Brien (1998) [31]	$\varepsilon_{sky,0} = 1 - e^{(-1.66\cdot\tau)} \quad \tau = 2.232 - 1.875\left(\frac{T_a}{273.15}\right) + 0.7356\sqrt{18.6\left(\frac{e_0}{T_a}\right)}$ $\varepsilon_{sky,0} = \frac{1}{\sigma\cdot T_a^4}\cdot\left[59.38 + 113.7\cdot\left(\frac{T_a}{273.15}\right)^6 + 96.96\sqrt{18.6\left(\frac{e_0}{T_a}\right)}\right]$	32, 33
Niemelä et al. (2001) [27]	$(e_0 \geq 2) \rightarrow \varepsilon_{sky,0} = 0.72 + 0.009\cdot(e_0 - 2),$ $(e_0 < 2) \rightarrow \varepsilon_{sky,0} = 0.72 - 0.076\cdot(e_0 - 2),$	25, 26
Tang et at 2004 [28]	$\varepsilon_{sky,0} = 0.754 + 0.0044\cdot T_{dp}$	27

2.1.2. Cloudy sky relations

Clear sky conditions do not happen all the time. The presence of clouds increases the incoming infrared atmospheric radiation compared to clear sky conditions. This is because clouds act like a blackbody emitter supplementing the waveband the atmospheric emission lacks of. Any cloud

which is visually opaque can be considered as a blackbody emitter at the temperature of the cloud base [7] and its radiative effect is to close the infrared atmospheric window. Thus, clear sky correlations must be modified to adjust the cloudiness.

According to its own observations, Ångström [33] proposed a relation to take into account the cloudiness (Eq. 34).

$$\text{Eq. 35} \qquad R = R_0 \cdot (1 - kW)$$

Eq. 34 is a cloud correction relation which is being applied to the emitted radiation from the earth surface, and also to the incoming infrared atmospheric radiation. A more logical relation has been proposed by Bolz (1949) [34]. This relation (Eq. 35) takes into account the cloudiness of the sky only on the incoming infrared atmospheric radiation.

$$\text{Eq. 35} \qquad R_{\downarrow} = R_{\downarrow,0} \cdot (1 + kW^2) \rightarrow \varepsilon_{sky} = \varepsilon_{sky,0} \cdot (1 + kW^2)$$

Centeno (1982) [22] proposed a correlation to estimate the clear-sky emissivity (Eq. 14) and also a relation to get the effective sky emissivity bearing in mind the cloudiness (Eq. 36).

$$\text{Eq. 36} \qquad \varepsilon_{sky} = \varepsilon_{sky,0} + W \cdot \left(\varepsilon_{cloudy\ sky} - \varepsilon_{sky,0}\right)$$

Kimball et al. (1982) [35] developed a method that assumes that the cloud radiation is transmitted through the air only at the infrared atmospheric window. The model (Eq. 37) takes into account the information obtained from every cloud layer.

$$\text{Eq. 37} \qquad R_{\downarrow} = R_{\downarrow,0} + \sum_i^N \tau_8 W_i \varepsilon_{cloud,i} f_{8,i} \sigma T_{c,i}^4$$

The authors also proposed a series of correlations to calculate these parameters.

Martin and Berdahl (1984) [24] proposed a relation that takes into account the cloud emissivity and the cloud-base temperature (Eq. 38).

$$\text{Eq. 38} \qquad \varepsilon_{sky} = \varepsilon_{sky,0} + \left(1 - \varepsilon_{sky,0}\right) \cdot W \cdot \varepsilon_{cloud} \cdot \Gamma$$

Sugita and Brutsaert (1993) [36] proposed new and more accurate values (Eq. 39) for parameters of a previous correlation (Eq. 35).

$$\text{Eq. 39} \qquad R_{\downarrow} = R_{\downarrow,0} \cdot (1 + u \cdot W^v) \rightarrow \varepsilon_{sky} = \varepsilon_{sky,0} \cdot (1 + u \cdot W^v)$$

Aubinet (1994) [37] proposed a correlation to estimate the effective sky temperature that takes into account the clearness index (Eq. 40).

Eq. 40 $$T_{sky} = 94 + 12.6 \cdot \ln(e_0) - 13 \cdot K_0 + 0.341 \cdot T_a$$

Crawford and Duchon (1999) [38] improved a previous correlation [19] (Eq. 30) to take into account the annual variation between dry and wet season and also proposed a relation for estimating the effect of cloudiness (Eq. 41).

Eq. 41 $$\varepsilon_{sky} = clf + (1 - clf) \cdot \left(1.22 + 0.06 \cdot \sin\left((month + 2) \cdot \frac{\pi}{6}\right)\right)\left(\frac{e_0}{T_a}\right)^{\frac{1}{7}}$$

$$clf = 1 - s$$

Sridhar et al. (2002) [39] modified a correlation from previous work [19] (Eq. 30) by calibrating it for different sites representing different climatic and geographical conditions to make it valid for all sky conditions (day and night; clear and cloudy) (Eq. 42).

Eq. 42 $$\varepsilon_{sky} = 1.31 \cdot \left(\frac{e_0}{T_a}\right)^{1/7}$$

Note that in Equation 42 e_0 must be used in mbar, in contrast to the original reference, where it is used in kPa (introducing a conversion factor in the equation).

Also, with overcast sky can be used previous presented radiative-transfer models/modelization (LOWTRAN, MODTRAN, SBDART), showing good agreement with pyrgeometer measurements [40]. Also, this work shows that cloud base height should be measured and taken into account.

All the relations that consider cloudy-sky just take into account the long-wave radiation. Under cloudy conditions short-wave radiation is reduced; however long-wave radiation is increased. Therefore, previous equations are not suitable when short-wave radiation needs to be calculated.

As proposed at the beginning of this section, some works conclude that clear-sky correlations underestimate the incoming infrared atmospheric radiation under cloudy conditions [36,38,41]. Also, in Table 2 is presented a summary of the correlations found in the literature for cloudy-sky conditions.

Table 2 Summary of cloudy-sky correlations.

Authors	Cloudy-sky correlations	Equation
Ångström [33]	$R = R_0 \cdot (1 - kW)$	34
Bolz (1949) [34]	$\varepsilon_{sky} = \varepsilon_{sky,0} \cdot (1 + kW^2)$	35
Centeno (1982) [22]	$\varepsilon_{sky} = \varepsilon_{sky,0} + W \cdot \left(\varepsilon_{cloudy\ sky} - \varepsilon_{sky,0}\right)$	36

Kimball et al. (1982) [35]	$R_{\downarrow} = R_{\downarrow,0} + \sum_{i}^{N} \tau_8 W_i \varepsilon_{cloud,i} f_{8,i} \sigma T_{c,i}^4$	37
Martin and Berdahl (1984) [24]	$\varepsilon_{sky} = \varepsilon_{sky,0} + \left(1 - \varepsilon_{sky,0}\right) \cdot W \cdot \Gamma \cdot \varepsilon_{cloud}$	38
Sugita and Brutsaert (1993) [36]	$\varepsilon_{sky} = \varepsilon_{sky,0} \cdot (1 + u \cdot W^v)$	39
Aubinet (1994) [37]	$T_{sky} = 94 + 12.6 \cdot \ln(e_0) - 13 \cdot K_0 + 0.341 \cdot T_a$	40
Crawford and Duchon (1999) [38]	$\varepsilon_{sky} = clf + (1 - clf) \cdot \left[1.22 + 0.06 \cdot \sin\left((month + 2) \cdot \frac{\pi}{6}\right)\right] \left(\frac{e_0}{T_a}\right)^{1/7}$	41
Sridhar et al. (2002) [39]	$\varepsilon_{sky} = 1.31 \cdot \left(\frac{e_0}{T_a}\right)^{1/7}$	42

2.1.3. Influence of the zenith angle / tilted surfaces / sky view factor

To maximise the effective outgoing infrared radiation, the radiator should be placed horizontally, facing the sky. However, sometimes it is desirable to install the radiator with an inclination, as for example to allow drainage or because it is the inclination of the roof where it is placed. The inclination of the radiator increases the incoming infrared radiation at radiator surface. This increase in the incoming radiation is mainly caused by the reduction of the sky view factor from the radiator surface (therefore, the surface is facing the ground which acts more likely to a blackbody), and also because the radiator's surface is more exposed to the "warmer" regions of the sky near the horizon (due to the less "visual thickness" of the atmosphere in the zenith direction [6] than in other directions).

As the effect produced by the variation of the view factor is easier to estimate than the effect of being exposed to "warmer" zones of the sky, research was mainly focused on finding simple expressions of the effect of having the radiator surface exposed to "warmer" regions of the sky, rather than the analytical expression of the phenomenon as presented in [4].

Some of the authors tried to establish correlations to relate the incoming infrared radiation or the effective outgoing infrared radiation to the inclination angle or the zenith angle. To express the variation of the net outgoing infrared radiation in relation with the zenith angle Linke (1931) [42] found an expression (Eq. 43) that adapts adequately to measurements from literature.

Eq. 43 $$R_0(\theta) = R_0(0) \cos^{\gamma} \theta$$

Eq. 44 $$\gamma = 0.11 + 0.0255 \cdot e_0$$

In a similar way, Strong (1941) [43], based on its own measurements of the angular dependence of clear-sky infrared radiation from the atmosphere, readapted a previous formula (Eq. 5) to take into account the zenith angle (Eq. 45).

$$\text{Eq. 45} \qquad R_{\downarrow,0}(\theta) = \left(a + b\sqrt{e_0 \cdot \sec\theta}\right)\sigma T_a^4$$

Based on Eq. 43 and Eq. 45, and from experimental measurements from the literature [5,42,43], it can be drawn that for angles smaller than $45°$ the effect of the deviation from the zenith angle is not significant (about 4 to 6% error [44]).

Other authors made some effort on searching good expressions that allow calculating the effect of inclination on the equivalent sky emissivity.

Granqvist and Hjortsberg (1981) [45] proposed an expression to relate the sky emissivity to the zenith angle (Eq. 46), considering the atmospheric transmittance proportional to the pathlength, which depends on wavelength and zenith angle.

$$\text{Eq. 46} \qquad \varepsilon_{sky,0}(\theta,\lambda) = 1 - \left[1 - \varepsilon_{sky,0}(0°,\lambda)\right]^{1/\cos\theta}$$

Eq. 46 relates the sky emissivity at zenith angle to any sky emissivity at any angle from the zenith, showing good agreement in the atmospheric window range when compared to LOWTRAN data (Figure 1).

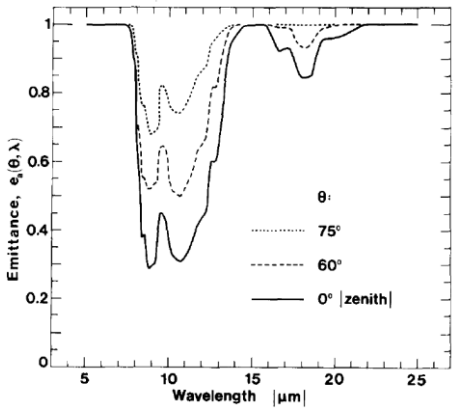

Figure 1 Spectral emittance of the atmosphere for three zenith angles as obtained from the radiance data computed from a LOWTRAN model [45].

As Eq. 46 performs well in the infrared atmospheric window, the "box model" was proposed [45], which consists of dividing the infrared range in three parts where each part has an emissivity according to Eq. 47.

Eq. 47
$$\varepsilon_{sky,0}(\theta,\lambda)=\begin{cases}\varepsilon_{sky,0}(\theta)=1 & 3<\lambda<8\ \mu m\\ \varepsilon_{sky,0}(\theta)=1-\left[1-\varepsilon_{sky,0}(0)\right]^{1/\cos\theta} & 8<\lambda<13\ \mu m\\ \varepsilon_{sky,0}(\theta)=1 & 13<\lambda<50\ \mu m\end{cases}$$

In a similar way, Martin and Berdahl (1984) [46] measured and studied the spectral and angular dependence of the sky radiation. Considering the atmospheric transmittance proportional to the pathlength and also making some approximations, they proposed a correlation (Eq. 48) that relates the equivalent sky emissivity with the zenith angle and the wavelength.

Eq. 48
$$\varepsilon_{sky,0}(\theta,\lambda)=1-\left(1-\varepsilon_{sky,0}\right)[t(\lambda)/t_{av}]e^{b(1.7-1/\cos\theta)}$$

Due to the low influence of zenith angle for small angles and the difficulty to calculate accurate correlations, no extended research had been conducted in this issue.

2.2. Radiative cooling potential (resource)

Radiative cooling as a technology is considered new and little tested. Before evaluating any device, the energetic and economic potential of the technology should be analysed. The main factors that determine whether to use this technology are the weather (meaning by weather the atmospheric conditions), and the cooling requirements of the building in the particular location. All work done until date is limited to taking into account the weather, but omitting the cooling requirements.

In the early research, Atwater and Ball (1978) [47] computed values of infrared atmospheric radiation from 11 USA meteorological stations (continental/subtropical climates) to create a model to estimate the average sky temperature. They also created some contour maps with the areal distribution of the sky temperature and the temperature depression (difference between ambient temperature and sky temperature) for each season, showing temperature depressions between $6-18$ degrees. Later on, Martin and Berdahl (1984) [24] calculated the radiative cooling potential in the USA using their own model. They presented some average monthly temperature depression maps, percentage maps (showing sky temperature below 16℃) and temperature depression histograms to characterise the radiative cooling resource. These results show up some climates to be more suitable to use radiative cooling than others, as for example Fresno's (California) climate.

The radiative cooling potential of a tropical country as Thailand, has also been analysed. Exell (1978) [48] used two methods to determine the potential in Thailand. The first method uses empirical correlations previously shown (Eq. 8 and Eq. 34), while the second method uses a theoretical equation of radiative transfer for atmospheric radiation [13]. Results show effective

sky temperatures about 8℃ below minimum daily temperature, demonstrating the potential of radiative cooling to provide some of the cooling demands. Moreover, Hanif et al. (2014) [49] performed an analysis of the radiative cooling potential for Malaysia. They attempted to get a correlation to relate the radiative cooling power and the temperature depression by using climate data from 10 different locations. The study found that the potential savings in Malaysia due to radiative cooling are up to 11% of cooling energy consumption.

Exploring another typology of climate, Pissimanis and Notaridou (1981) [50] calculated the radiative cooling potential in Athens (Subtropical/Mediterranean) during summer using the model proposed by Atwater and Ball [47]. Their results were corroborated with 7 years of measurements and 2 empirical correlations (Eq. 5 and Eq. 8). In the same way, Argiriou et al. (1994) [51] calculated the radiative cooling potential also in Athens, using 12 years of hourly weather measurements. Argiriou et al. (1994) used Berdahl and Martin (1984) [23] model to calculate the sky emissivity. They presented sky-temperature depression histograms, cumulative frequency distribution of the stagnation temperature graphs, and cumulative frequency distribution of the outlet temperature with or without wind screen graphs, concluding that the location is suitable to apply radiative cooling techniques.

After initial research in assessing radiative cooling potential, Burch et. al. (2004) [52] presented a new insight by taking into account the energy demand coverage of a standard building when assessing radiative cooling potential in a specific location. It was used a model to predict the energy production and energy demand coverage, space heating and cooling and domestic hot water, for a building located in Albuquerque, Madison and Miami (USA). Overall results of energy demand coverage and money savings were presented for each city.

Very little is done in evaluating the potential of the technology and also very few climates had been evaluated. More research is needed to evidence which climates are meaningful to implement this technology according not just to the weather conditions but also to the cooling requirements.

In conclusion, a world climate analysis should be performed in order to determine where this technology may be implemented and how well can it perform. However, as radiative cooling is a new technology, some parameters should be standardized.

3. Selective radiative cooling

The net thermal balance between a terrestrial surface and its surroundings determines the surface temperature. Radiative cooling takes into account radiative properties of the atmosphere to generate a net cooling thermal balance. To take advantage of the infrared atmospheric

window, some authors proposed the use of selective materials with specific optical properties, in order to achieve lower surface temperatures by emitting mainly in the infrared atmospheric window [53–56]. These optical properties should ideally be those of a perfect emitter in the infrared atmospheric window (8-13 μm) and a perfect reflector elsewhere. In this case the cooling power is on the order of $100\ W/m^2$ at ambient temperature, and temperatures around 50℃ below ambient temperature could be reached (considering radiation balance only) [57].

A perfect material for radiative cooling applications does not exist, but some research has been conducted in order to determine the optical properties of existing materials and also to create new materials with better properties.

Selective properties can be achieved by using a selective surface, but they can also be achieved by using a selective screen, which can at the same time block the convection heat transfer between the cold surface and the ambient air, as well as reflect some unwanted radiation. A combination of a selective surface and a selective screen can also be a solution. If a cover screen is used, there is also the possibility to replace the air between the radiator surface and the cover screen with another gas with more desirable radiative properties or create vacuum. Moreover, the use of mirrors to focus the radiation of a specific zone from the sky is also seen as a potential improvement.

In this section, research and advances in selective materials for radiative cooling are reviewed, classified and discussed. The main classifications for the materials, bearing in mind their specific position in the device, are: surface of the radiator, cover for the radiator, gas between cover and surface, and auxiliary systems (as mirrors).

3.1. Selective surface

Some research has been conducted on this topic trying to find a suitable material or coating to enhance radiative cooling. The aim is to develop an ideal material with high emissivity in the infrared atmospheric window wave range (8-13 μm) and high reflection in the remaining wavelengths.

To optimize and compare selective surfaces for radiative cooling applications, some parameters are defined [45] in order to represent the potential of the selective surface. This parameters are: the average emissivity for different wavelengths ranges ($\bar{e}_s^H$ and $\bar{e}_{s,2}^H$) (Eq. 49 and Eq. 50) and a new comparative parameter (η^H) (and Eq. 51):

$$\text{Eq. 49} \qquad \bar{e}_s^H = \int_0^\infty I_{b,\lambda}(\lambda, T_s) \cdot [1 - \rho(\lambda)\,] \cdot d\lambda \,/\, \int_0^\infty I_{b,\lambda}(\lambda, T_s) \cdot d\lambda$$

Eq. 50 $$\bar{e}_{s,2}^{H} = \int_{8\mu m}^{13\mu m} I_{b,\lambda}(\lambda, T_s) \cdot [1 - \rho(\lambda)\,] \cdot d\lambda \,/\, \int_{8\mu m}^{13\mu m} I_{b,\lambda}(\lambda, T_s) \cdot d\lambda$$

Eq. 51 $$\eta^{H} = \bar{e}_{s,2}^{H} / \bar{e}_{s}^{H}$$

Eq. 49 is the average emissivity of the material, Eq. 50 is the average emissivity of the material between $8 - 13\mu m$ wavelenghts and indicates the maximum achievable cooling power, and Eq. 51 is a comparison parameter between the previous two parameters and indicates the maximum achievable temperature drop. Therefore, high values of $\bar{e}_{s,2}^{H}$and η^{H} are desired. These parameters appear in some of the works presented below to discuss and analyse the feasibility of the selective surfaces.

These selective surfaces can be obtained by means of Polymer foils on metal surfaces, Silicon-based coatings on metal surfaces, Ceramic oxide layers, Paints and New Materials (multilayers).

3.1.1. Polymer foils on metal surfaces

In the search of a selective surface for radiative cooling applications, polymer foils on metal surfaces (highly reflective) have been tested, mainly on aluminium. Three different polymers were analysed (polyvinyl-chloride (PVC) [58], polyvinyl-fluoride (PVF-TEDLAR) [53–55] and poly 4-methyl-1-pentene (TPX) [59]), and had been also compared to each other [45]. Results of the comparison between the three polymers can be seen in Figure 2.

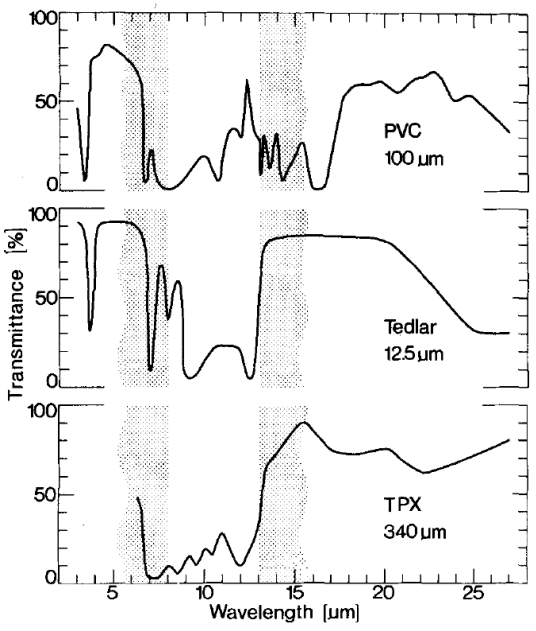

Materials	Thickness (μm)	$\bar{e}_{s,2}^{H}$	η^{H}
PVC	50	0.78	1.2
Tedlar	12.5	0.84	1.6
TPX	340	0.89	1.6

Figure 2 Left: Transmittance spectra for three different plastic films. Right: Table of cooling parameters estimated for plastic films backed by aluminium [45].

These results show that the three polymer foils present a low reflectivity in the infrared atmospheric window (consequently high emissivity) but do not show such a good performance outside it. When compared with SiO films, the polymer foils show a better performance in the infrared atmospheric window but worse reflectivity outside the window, therefore, polymer foils show worse overall performance [45].

Polyvinyl-difluoride (PVDF) was also proposed as selective material for radiative cooling applications but only when used also in solar collection [60]. Even though the radiative performance was not as good as other selective materials, it performed better than non-selective surfaces.

In a recent work [61], where solar heating and radiative cooling were required, polyethylene terephthalate (PET) coated with titanium (Ti) was studied (called TPET by the authors), showing selective properties in the infrared window and also in the solar band, as shown in Figure 3.

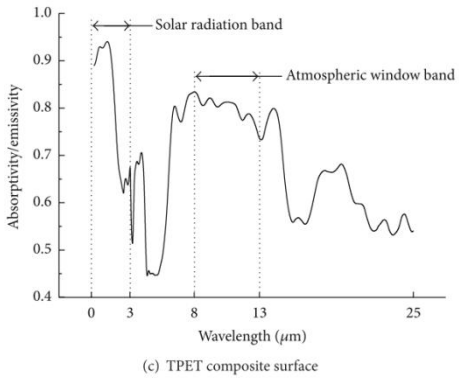

Figure 3 Spectral absorptivity (emissivity) of TPET composite surface [61].

3.1.2. Silicon-based coatings on metal surfaces

Several authors have studied the use of thin silicon-based coatings. The idea was to coat highly reflective metals, as aluminium, with silicon coatings which selectively emit in the infrared atmospheric window.

Silicon monoxide (SiO) is a coating that shows good performance. The reflectance and transmittance of Si on transparent $KRS-5$ and the reflectance of SiO films on aluminium substrates were studied by Hjortsberg and Granqvist (1980) [62] (Figure 4).The purpose of their research was to provide accurate knowledge of the optical properties over the whole thermal

infrared range. They conclude that their measurements are similar to what is found in the literature, so they endorsed results pointed out in previous works.

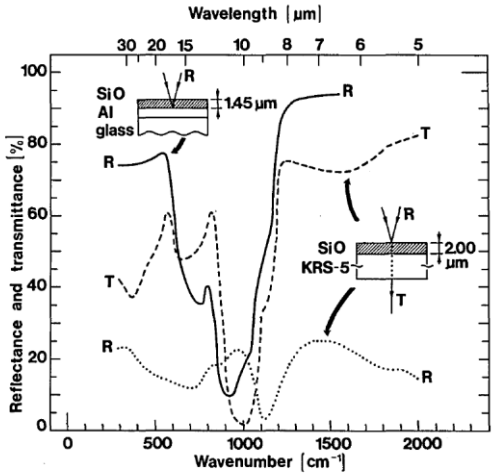

Figure 4 Spectral infrared reflectance and transmittance for evaporated SiO films [62].

Also, Granqvist et al. (1982) [57] tested SiO films on aluminium for different thicknesses (Figure 5 Left). In this research was compared a SiO film on aluminium to a black painted plate. The selective surface reached $14°C$ below ambient whereas the black plate reached slightly lower temperatures. The reason for this small difference between the selective surface and the black plate lied in an unfavourable low value of $\bar{e}_{S,2}^{H}$ for the SiO coating and an insufficient thermal insulation of the test box.

Moreover, Granqvist et al. (1982) [57] also studied Si_3N_4 films on aluminium (Figure 5 Right), showing better performance than SiO coatings according to the greater infrared atmospheric window range covered.

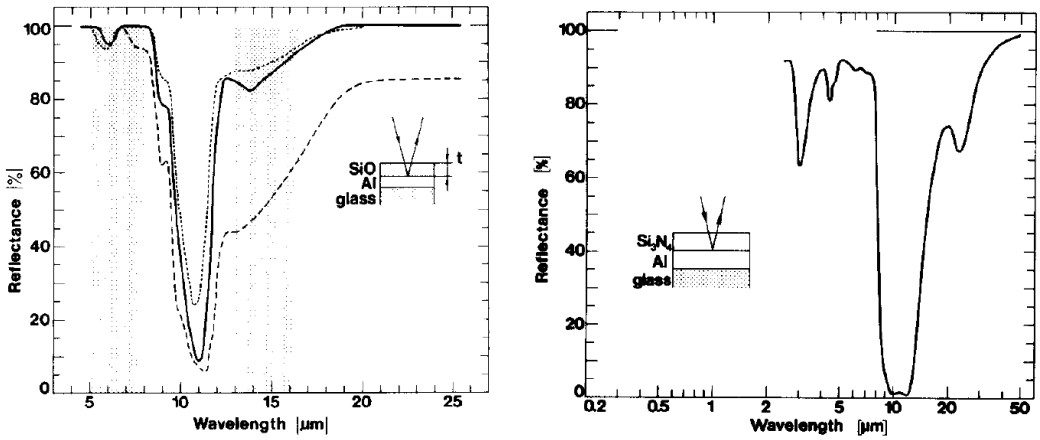

Figure 5 Left: Measured spectral reflectance for SiO/Al films on glass with three SiO film thicknesses [57]. Right: Measured spectral reflectance for an Si_3N_4/Al film on glass [57].

Another coating, $SiO_{0.6}N_{0.2}$, was tested by Eriksson and Granqvist (1983) [63] and by Eriksson et al. (1984) [64], showing better performance than SiO but worse than Si_3N_4 . Nevertheless, it showed suitable properties for radiative cooling (Figure 6).

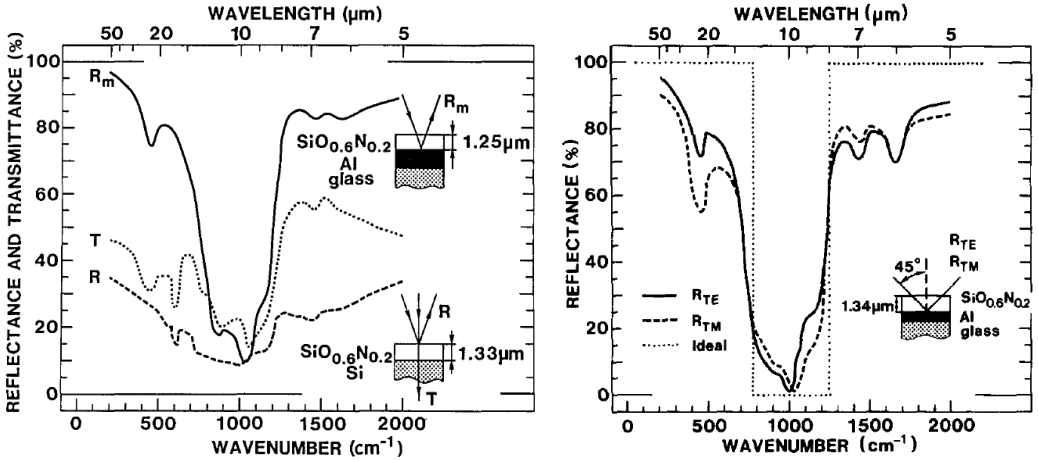

Figure 6 Left: Spectral reflectance and transmittance of evaporated $SiO_{0.6}N_{0.2}$ films on two different substrates [63]. Right: Spectral reflectance for a film of $SiO_{0.6}N_{0.2}$ deposited onto Al [64].

A bilayer coating of $SiO_{2.0}/Si0_{0.25}N_{1.52}$ on Al was also analysed by Eriksson et al. (1985) [65], showing a worse performance regard to $SiO_{0.6}N_{0.2}$ coating (Figure 7).

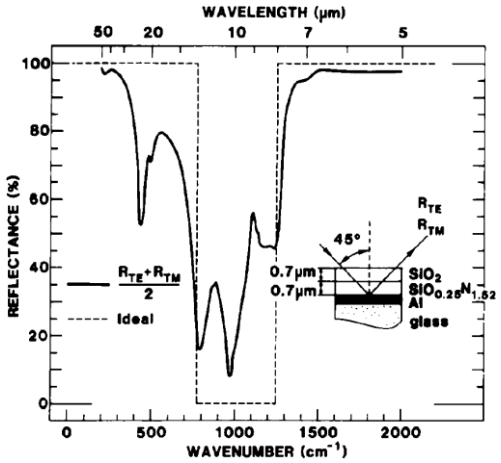

Figure 7 Computed spectral reflectance of $SiO_{2.0}/Si0_{0.25}N_{1.52}$ coating on Al [65].

The performance of a multilayer coating of SiO_xN_y using different concentrations of oxygen and nitrogen was measured by Diatezua et al. (1995) [66] (Figure 8). The authors pointed out that the performances of the analysed multi-layered samples are far from the perfect selective material. Moreover, their results are even worse than other single layer materials [53,65].

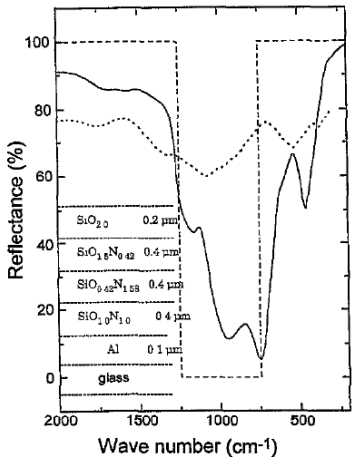

Figure 8 Reflectance measured for the sample represented on the figure [66].

Another configuration using a SiO film as outer layer consisting of vanadium dioxide (doped with tungsten or not) ($V_{1-x}W_xO_2$), a thermochromic film, as intermediate layer, and a blackbody surface as base, was numerically studied by Tazawa and Tanemura [67] and Tazawa et al. [68].

Transition metal oxide thermochromic films, like $V_{1-x}W_xO_2$, show optical switching behaviour corresponding to the phase transition from metallic to semiconductor at a certain temperature. Thermochromic materials have a high reflectance in the high temperature phase and low reflectance in the low temperature phase. Due to the fact that spectral selectivity only appears at higher temperatures, as seen in Figure 9 (left), it provides an automated temperature control of the surface.

Vanadium dioxide films (doped with tungsten or not) are candidate materials because the transition temperature of Vanadium dioxide (around $68°C$) can be reduced down below room set point temperature by adjusting the doping level. These works [67,68] present results of radiative cooling power and temperature stability of sky radiators for different doping level of tungsten.

Although these configurations do not show better performance than SiO/Al configurations, as can be seen in Figure 9 (centre), they present higher temperature control and stability as can be seen in Figure 9 (right) [68].

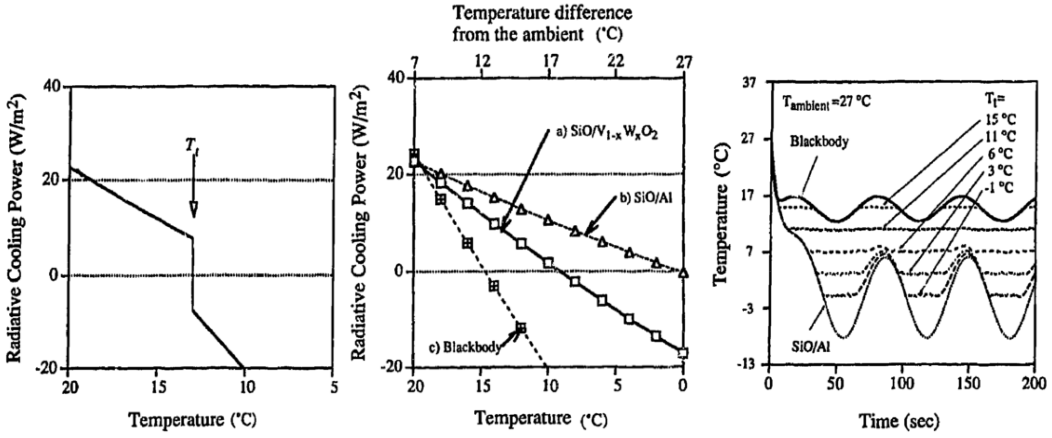

Figure 9 Left: Radiative cooling power of the sky radiator with respect to the phase transition of the thermochromic film [67]. Centre: Calculated radiative cooling power of the three different sky radiators[67]. Right: Temperature changes of the spectral selective radiating material [68].

3.1.3. Ceramic oxide layers

Another possibility to achieve radiative cooling to low temperatures is to use materials with high values of reflectivity at high wavelengths ($\lambda > 13\ \mu m$) instead of using high reflective materials all over the spectrum and coat it with high emissive materials at the infrared atmospheric window.

Magnesium oxide (MgO) ceramic samples have been studied [69] (Figure 10) and their behaviour has been compared to white painted surfaces, showing the first ones a better performance. MgO can reach lower temperatures than selective surfaces based on polyvinyl-fluoride (PVF), and has a high solar reflectivity which may allow radiative cooling with daylight.

Lithium fluoride (LiF) is also considered a good material for radiative cooling due to the similar optical properties at the infrared region as MgO [69] (Figure 10). Furthermore, it has also been suggested to manufacture selective radiators with LiF/MgO mixtures.

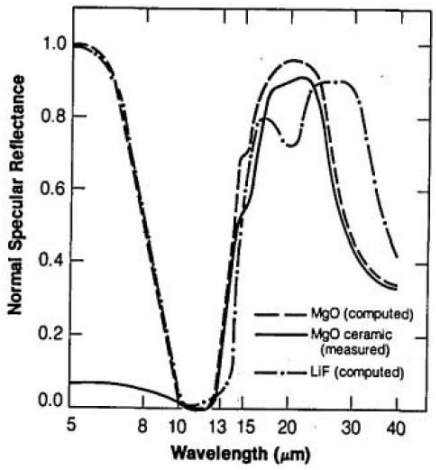

Figure 10 Computed normal specular reflectance for layers of MgO and LiF backed with a reflecting layer, and normal specular reflectance of a polished MgO ceramic sample [69].

3.1.4. Paints

In hot regions, white paints are commonly used when painting buildings in order to reflect solar radiation. Furthermore, the use of additives to enhance painting performance has been tested in order to provide high emissivity at the infrared atmospheric window. Therefore, the combination of white paints with these additives provides both high emissivity at the infrared atmospheric window and high reflectivity of solar radiation. White paints with some concentration of TiO_2 were tested (on aluminium plate) by Harrison and Walton (1978) [70] showing that high concentrations of TiO_2 (35%) can cool down 15℃ below ambient temperature in Calgary, Canada.

In the same way, Awanou (1986) [71] developed a diode roof system that had a pebbled roof with white paint with TiO_2 in order to reduce absorption of solar radiation and to emit radiation

during the night. The results were not as good as expected but better results are foreseen for hot and dry climates with long nights ($> 8h$).

Two other white pigmented paints based on $TiO_2/BaSO_4$ and TiO_2/ZnS were analysed by Orel et al. [72] showing that the addition of $BaSO_4$ improves the performance of radiative cooling.

3.1.5. New Materials (multilayers)

Recently, new manufacturing techniques allowing the development of new materials have been developed. These new materials are nanoscale multilayer combinations of materials, optimized to have better optical properties for radiative cooling.

Two new multilayer combinations of materials have been tested. The first one made of several layers of titanium dioxide TiO_2 and magnesium fluoride MgF_2 on silver cover with silicon carbide SiC and quartz [73], and the other consisting of alternating layers of silicon dioxide (SiO_2) and hafnium dioxide (HfO_2) on top of silver and silicon [74]. Both of them showed a good performance even under sunlight due to its high reflectivity of solar radiation and high emissivity in the infrared atmospheric window, as can be seen in Figure 11.

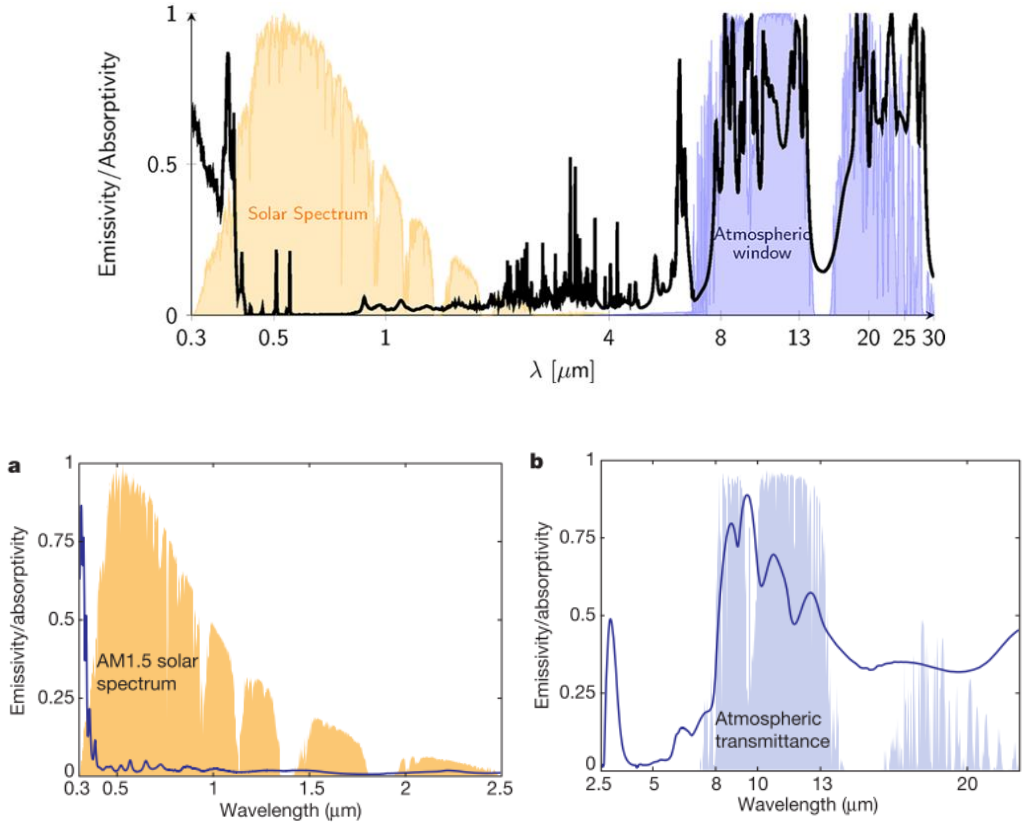

Figure 11 Up: Emissivity of the optimized daytime radiative cooler [73]. Down: Measured emissivity of the photonic radiative cooler [74].

3.2. Selective screen and convection shield

Due to the difficulty of achieving a material with perfect properties for radiative cooling and also reduce convection heat gains, the use of selective screens is proposed.

3.2.1. Polyethylene (PE)

First attempts in using convection shields [53–55,57,64,69,70] were conducted with polyethylene (PE) foils due to their good transmittance almost all over the spectrum (Figure 12). Due to its high transmittance at the infrared atmospheric window (85% [75]) it could be complementary to a selective surface radiator.

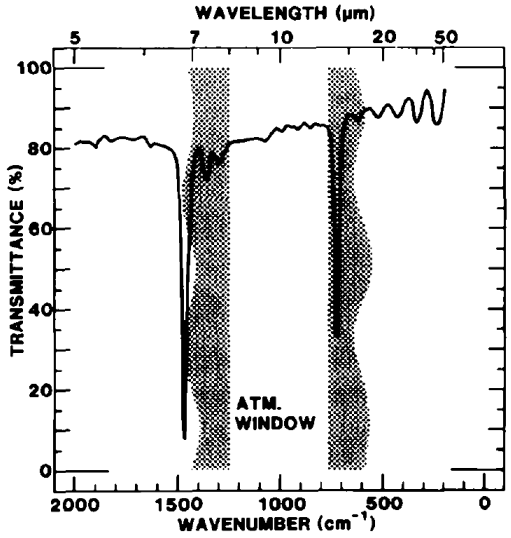

Figure 12 Normal spectral transmittance of a 30 μm thick foil of high-density polyethylene [75].

Different configurations were analysed instead of flat screens, as for example a V-corrugate screen design of high-density polyethylene (HDPE) foils (Figure 13, [75]). A better performance than a flat screen was observed when analysing its transmittance and thermal insulation as a convection shield.

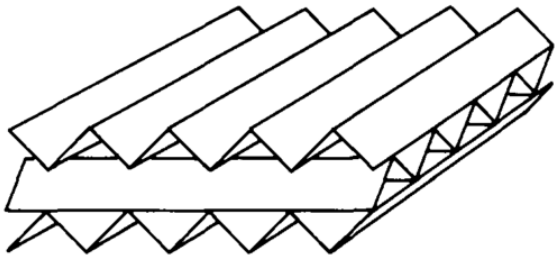

Figure 13 Sketch of the material with high infrared transmittance and low non-radiative heat exchange [75].

For a better understanding of polyethylene performance as a convection shield and selective screen, Ali et al. (1998) [76] studied the effects of aging, thickness, and colour on both the radiative properties of polyethylene films and the performance of the radiative cooling system, highlighting the poor aging of polyethylene foils. The authors also concluded that thinner films present a better performance in terms of night sky radiation, but worse mechanical properties. Moreover, the colour of the film does not significantly affect its optical properties. In a recent research a polymeric mesh has been proposed as a solution for structural weakness of PE [77]. However, although the authors (Gentle et al.) state that this configuration could extend the PE film life span to more than five years, they do not provide any data to support this statement, and do not analyse any potential optical properties degradation.

In order to reduce solar gains and increase the longevity of polyethylene foils several researches have been conducted, analysing different types of coatings. Nilsson et al. (1992) [78] studied zinc sulphide (ZnS) coating on low-density polyethylene (LDPE), showing a good solar reflectance and also a good transmittance in the infrared atmospheric window. This coating enables radiative cooling during the night and reduces heating under direct sunlight. Later on, Nilsson and Niklasson (1995) [79] described the optimization of optical properties and simulations of thermal performance during the day for pigmented polyethylene foils. The simulated pigment materials were ZnS, $ZnSe$, TiO_2, ZrO_2, and ZnO. Simulations showed that ZnS is the best of the pigmented materials tested for a cover foil.

Similarly, Mastai et al. (2001) [80] studied the optical properties of a coating of TiO_2 on polyethylene for different thicknesses, showing favourable optical characteristics, high reflectance in the solar band, and high transmittance in the atmospheric window band.

Low ban gap semiconductors (Te, PbS, and $PbSe$), are expected to block solar radiation, while being transparent in the infrared region. Engelhard et al. (2000) [81] studied semiconductors of

Te on polyethylene foils, exhibiting suitable characteristics for radiative cooling, high transmission in the mid-IR region, and high solar blocking. In the same way, Dobson et al. (2003) [82] studied the performance of semiconductor coatings of PbS and $PbSe$ on polyethylene foils, showing that combined with pigmented polyethylene foils of ZnS and ZnO they can provide optical and radiative cooling properties.

3.2.2. Other convection covers

Benlattar et al. (2005) [83] described the use of thin film $CdTe$ onto Silicon substrate by measuring its optical properties. $CdTe$ thin film is suitable for radiative cooling due to its low reflectance and high transmittance in the atmospheric infrared window. Moreover, Benlattar et al. (2006) [84] also described the use as selective cover of CdS, showing good optical properties for radiative cooling.

Mouhib et al. (2009) [85] studied stainless steel deposited on a tin coating layer and on a float glass sheet, as a selective screen over a blackbody emitter. This screen has negligible transmittance so it has a different behaviour in each side. The overall behaviour is that the upper face prevents the transmission of the greatest part of radiation coming from the sky, and allows the lower face to evacuate most of the thermal radiation emitted by an underlying material. The energy balance indicates that this configuration would be suitable for radiative cooling device based on spectral selectivity. Direct measurements confirmed this conclusion.

Bathgate and Bosi (2011) [86] analysed and tested experimentally the use of polyethylene and zinc sulphide as selective covers. They concluded that both covers perform similarly in thermal aspects, such as heat loss and radiative power, but mechanical/structural properties and durability of ZnS are much better, making it a more suitable material. Finally, they also mentioned the high price of ZnS glass and suggested that a much cheaper way to manufacture zinc sulphide screens should be developed to make it affordable to be used as cover.

3.3. Gas slab

Another point to take into account is the air gap between the cover and the radiator plate. Little research has been conducted in the study of optical properties of certain gases to emit through the infrared atmospheric window. These gases should emit/absorb mainly in the infrared atmospheric window but transmit elsewhere.

The main gases studied for this purpose are ethylene (C_2H_4) [64,87–89], ethylene oxide (C_2H_4O) [64,88,89] and ammonia (NH_3) [64,88–90].

Lushiku and Granqvist (1984) [89] presented a concise summary of the research conducted in this topic, identifying ethylene (C_2H_4), ethylene oxide (C_2H_4O) and ammonia (NH_3) as proper gases for radiative cooling. They measured the optical properties of these gases for different thicknesses and also computed and analysed the cooling capacity of the three gases as well as for mixtures of ethylene and ethylene oxide. Finally, they tested ethylene and ammonia as infrared selective gases in a simple radiative cooling device. The experiment showed the cooling effect but did not demonstrate its full potential. They concluded that ammonia was preferred when larger cooling power is required at near-ambient temperature, whereas mixtures of ethylene and ethylene oxide allow cooling to lower temperatures.

3.4. Directional selectivity

Part of the research in this topic has been conducted in analyse the behaviour of the radiator when using parabolic mirrors or in analyse how to control the direction of the incident/outgoing radiation. Such approaches are based on perfect reflector materials acting as mirrors; therefore, the system and not the material is analysed.

Du Marchie van Voorthuysena and Roes (2013) [91] proposed the use of parabolic mirrors to produce radiative cooling effect, even in daytime, by focusing the mirrors to a low effective temperature part of the sky . This concept is based on the adaptation of a parabolic solar collector for this purpose, so these collectors could produce both effects. The purpose of the research was to find out if radiative cooling and wind cooling have enough power to cool down large parabolic trough solar power stations. They conclude that there exists such potential to be used but occasionally supported by additional cooling.

Another research [92,93] proposed the use of Compound Parabolic Concentrator (CPC) technology to improve the radiative cooling effect focusing the radiator to the lowest effective temperature part of the sky. CPCs allow absorbing radiation coming from just a specific part of sky, reject all emitted radiation from other parts of sky and also reject all radiation emitted by the radiator. This technology could provide up to $135\ W/m^2$ at $10°C$ below the ambient [93].

4. Theoretical approach and numerical simulation

Some authors have conducted their research in theoretical approaches of radiative cooling phenomenon and in simulating them. Also, numerical simulations are suitable tools for the design and evaluation of radiative cooling systems. Moreover, several authors have focussed their research in the development of numerical models capable to accurately simulate radiative cooling systems. In this section, these models are reviewed and compared in order to identify research needs for improvement.

When analysing radiative cooling devices, the radiator plate is the main part of the device. Most authors modelled the radiator plate in a similar way as a solar flat-plate collector that, instead of gaining heat from the Sun, loses heat toward sky.

Most solar collectors have a cover to reduce the heat losses. However, in radiative cooling devices, losses are beneficial, therefore, for particular weather conditions, the cover is not desired. For instance, if ambient temperature is lower than the radiator one, using cover is a disadvantage. Otherwise, using a cover when ambient temperature is higher than the radiator temperature avoids undesired heat gains.

The thermal behaviour of the radiator is influenced by the heat transfer between the radiator and the surrounding media (sky, ambient, and internal fluid). Most of the authors consider at least the sky and the ambient when performing simulations to assess the potential of the device.

The most challenging effect to model is the influence of the sky, especially when the radiator is covered with a screen. Nevertheless, first attempts [94–99] considered the use of a screen. They presented analytical approaches combined with optical transmittance profiles of the screen and the sky.

Most recent works [73,74,100–114] on simulation either did not consider a cover or omit its influence. In these works the sky influence is treated in two ways: having it an effective temperature determined with empirical correlations [100–114] or considering the sky to have a wavelength dependant emittance and treat it analytically [73,74].

Not using a cover on the radiator plate simplifies the model of the radiative cooling device. However, if low temperatures are required, the use of a cover is necessary to reduce heat transfer from the ambient.

Another effect is the influence with ambient which is mainly by convection. When analysing convection between the device and the ambient is more difficult when there is a cover. This is due to the additional phenomena involving the air between the radiator surface and the cover that must be taken into account. Even that, it is difficult to determine the convection heat transfer coefficient in both cases. So, to deal with it, some authors [73,74,95] used parametric analysis with different convection heat transfer coefficients, in order to avoid to calculate for every condition, and to provide enough information to present some conclusions.

Finally the influence of the internal fluid with the radiator temperature for some authors it is considered in different ways: function of the accumulation tank temperature or conditioned

space temperature [101–104,108,109,111–113], simulated with CFD [105], or not used (just calculated the maximum reachable temperature) [95,96,73,74].

There exists a formula (Eq. 52) that gathers the overall of the effects and gives the fluid temperature at any point of a solar collector when operating at steady state [115]:

$$\text{Eq. 52} \qquad \frac{T_f - T_a - S/U_L}{T_{fi} - T_a - S/U_L} = e^{\left(-U_L \cdot n \cdot w \cdot F \cdot y \,/\, \dot{m} \cdot C_p\right)}$$

Where T_f is the temperature of the fluid at the desired point (normally the outlet fluid temperature), T_{fi} is the inlet fluid temperature, T_a is the ambient temperature, S is the radiation absorbed by the solar collector, U_L is the overall heat loss coefficient, n is the number of parallel tubes, w is the distance between parallel tubes, F is the collector efficiency factor, y is the tubes length, $\dot{m}$ is the mass flow rate and C_p is the specific heat of the fluid. This equation is for solar collectors. Readapting it for a radiator plate by replacing the solar heat gain for the net radiative heat loss was used by some authors [100–103,106–108,110,114] to predict the outlet fluid temperature.

The research conducted in this topic has now been introduced according to its influence to surroundings. From here on, conclusions from their authors are presented.

First approaches of radiative cooling devices showed that this technology could be used to provide part of the cooling demand of a building (50% cooling demand [94]), achieving promising values of net cooling power and reaching temperatures far below ambient ($65\ W/m^2$ - $\Delta T \geq 10K$ [95] and $60\ W/m^2$ - $\Delta T = 14K$ [96]). Also, some of this research has been conducted in hot and arid areas (Jordan) [98] modelling a radiative cooling device and validating it with empirical data showing good correlation and also good results (reducing the temperature of a $120L$ tank to $15°C$ in a night, $13MJ/m^2 \cdot night$). Later on, the same authors used this device to improve a previous nocturnal cold storage [99], presenting some conclusions about its dynamic thermal behaviour.

Recent research [73,74] computed selective materials with photonic design optimization, showing that this new combination of materials can produce cooling (up to $100\ W/m^2$ [73]).They also demonstrated that cooling can be achieved even under daylight conditions, reaching experimental values of $40\ W/m^2$ of cooling power [74].

The coupling between radiative cooling and photovoltaic solar collection [109] was also studied. After validating the model with empirical data, it was used to perform an analysis of its

performance in two cities, Madrid and Shanghai. The cooling annual potential calculated is of 51 and 55 kWh/m^2year for each location.

Some research [101–103] studied multistep refrigeration systems combining radiative cooling with evaporative cooling for climate conditions in Iran. Their model has been validated with the results from [116].The potential of the radiative cooling device was investigated for four cities showing that can be provided air up to $16K$ below ambient temperature and when combined with evaporative cooling up to $24K$ below ambient temperature, entailing savings up to 80% of the total cooling demand.

A research combining radiative cooling with microencapsulated phase change material [104], was simulated in five typical cities across China also showing great performance with savings up to 77% of the total cooling demand.

The one using CFD to simulate radiative cooling devices do not show good results if only is considered the thermal radiation (up to 20 W/m^2 [105]). Maybe, this is because the thermal radiation is calculated in a chosen steady state by the author that may not represent the reality.

An air-based system tested in a building in Greece [108], using an aluminium painted tube set to work as a nocturnal metallic plate radiator, was used to validate an analytical model showing good agreement.

A model using water as inner fluid and using general heat transfer equations was proposed [110]. The model was validated with experimental data with statistical methodology of analysis. The model showed uncertainty less than 5% when validated with data under experimental conditions showing experimental average powers of 60 W/m^2.

The combination of solar heating and radiative cooling, as passive system, has been simulated to condition the interior temperature of a building [111]. Savings up to 54% of heating and 53% of cooling can be achieved.

Some of the numerical simulations, validated with experimental data, were used to determine the effects of different parameters on the performance of the radiative cooling device, such as fin efficiency factor, flow rate, and overall heat transfer coefficient in [106,107,114], area/volume tank ratio, flow ratio, tank volume, and radiators surface in [116], and flow rate in [112,113]. In [107] are presented some different required characteristics between radiative cooling radiators and solar flat plate collectors used for solar heating. The authors concluded that fins used in flat plate solar collectors are less efficient for cooling applications, and an appropriate solution is radiators consisting entirely of pipes. Moreover, previous experimental

data [114] was also used to validate a research [112] which also assess the influence of the flow rate in the model performance.

After analysing all research done in theoretical approach and numerical simulations of radiative cooling devices it can be seen that great effort has been done since the first attempts in testing new aspects that improve its performance and applicability.

5. Radiative cooling prototypes

Part of the research has been conducted in testing experimental radiative cooling devices under certain circumstances. Most of this research has been done in order to provide experimental data to validate numerical models and to experimentally analyse the thermal behaviour of the prototypes. Most of the prototypes have the same shape as a solar collector, a flat plate as radiator.

First attempts [71,117] aimed at providing a roof which could produce some cooling during night and reflect the incident solar radiation during day. Air based systems were used to cool down the temperature of huts where were tested. In [117] 2 different covers were compared, galvanised steel painted white and aluminium coated with Tedlar. Both cases provided low cooling powers ($22\ W/m^2$), showing better performance the painted one, which reached lower temperatures (6℃ below ambient temperature during night).In [71] a new concept called diode roof was tested. Although this concept allows reaching lower temperatures than ambient during night, the main purpose was to avoid the heat to go inside the building.

Another type of air-based system was tested in a building in Greece [108], using an aluminium painted tube set to work as a nocturnal metallic plate radiator. This study was performed in two different offices, one office using a radiative cooling and the other one with no cooling device. The system operation is to pass interior air through the tube to be cooled down before reintroduce it inside the room during night hours. Experimental results showed that the office using radiative cooling achieved temperatures between $2.5 - 4$℃ below the one with no cooling device. Two different paints were tested, demonstrating the importance of a high emissivity of the radiator to achieve lower temperatures. Moreover, a numerical model was developed and experimentally validated.

Later research focussed in the use of high heat capacity transfer fluids, as water, because water-based systems can be better controlled and operated. Water-based systems can either be open or closed. Open water-based systems combine evaporative cooling, radiative cooling and

convective cooling. However, water is in contact with ambient, therefore it can evaporate and the system may need refilling. One of the first open water-based systems was developed by Dan and Chinnappa (1989) [118]. They used a solar collector where water was trickled over the cover glass during the night and 400L of heated water were cooled down almost to the diurnal minimum temperature. Another purpose of open water-based systems is to use water to clean and remove the dust from the collector cover.

To avoid losing water and catching dust in the water, the majority of water-based systems are closed systems. A closed water-based system was used by Matsuta et al. (1987) [60] who were some of the first authors to combine and evaluate solar heating and radiative cooling using a solar collector. They showed that, even this combination does not perform as well as they do separately, it could provide a good heating and cooling power (up to $610W/m^2$ $-51W/m^2$ respectively).

In a similar way, Ezekwe (1990) [119] tested a radiative cooling device to cool down a small refrigerator to store food and other perishable goods in developing countries and in remote areas. The system provided an average cooling capacity of $628kJ/m^2night$ and reached temperatures 7℃ below ambient.

Bearing in mind that the thermal demand of cooling is required during day time and the cooling is obtained during night; the use of thermal storage is needed. Ito and Miura (1989) [120] started using sensible thermal storage in combination with radiative cooling. An experimental and theoretical investigation of an uncovered radiative cooling radiator was performed. Results showed cooling powers of $40-60W/m^2$ in clear summer nights and $60-80W/m^2$ in winter, with thermal storage temperatures $2-5$℃ below ambient temperature.

Later on, a Erell and Etzion did a series of experiments in Israel about how radiative cooling performs in this hot and arid weather [106,107,121–123]. First experiment was set to determine the effect of the thermal storage mass in radiative cooling plate [121]. Four test boxes including an internal concrete slab at different locations were tested, trying to show the influence of this slab with the heat transfer by natural convection. The authors stated that the thermal storage mass has the role of being a heat sink and also of preventing the radiator to have lower temperatures than the design temperature of the cooled space. The authors concluded that the existence of a thermal storage mass is a very important part of a cooling system but even more important is the location of the thermal mass and the coupling between it and the radiating surface.

Later on, the same authors set an experiment using water as heat exchange medium [122]. The experiment was performed using a test box similar to those used in [121] which was adapted to a solar collector (without glass) by adding a roof pond and a pumping system. The effect of the water flow rate was tested, showing that it affects the temperature difference between radiators inlet and outlet temperature. So, in this sense, the emerged hypothesis that a higher flowing rate increases the cooling rate was not supported by the data. The authors concluded that this is a self-regulated system, in the sense that higher daytime heat loads results in higher night-time cooling rates. Moreover, the amount of water in the pond is an important parameter; it can be used to regulate the radiator temperature in order to achieve a suitable temperature for cooling purposes when needed as well as an acceptable cooling rate during night. Finally, they found that the coupling of the radiator with the thermal mass of the building results in higher temperatures than ambient air, making it possible to take advantage of convective cooling. This feature of the system obviates the need for wind screens, which previous research demonstrated that are essential for achieving low radiator temperatures. For this prototype, the cooling potential, taking into account convective and radiative cooling, was up to 90 W/m^2.

Additionally, Erell and Etzion used this previous radiative cooling device to test it as a solar heating collector [123], resulting in a considerable heating output (mean daily heating rate 1.94 kWh/m^2day), although it was not designed for such use. Finally, the authors proposed an analytical formulation to simulate a radiative cooling device based on a solar collector analysis [106,107,114]. The model was experimentally validated, showing good agreement.

In a similar approach, Meir et al. (2002) [116] tested an unglazed radiator, using water as a heat transfer fluid, coupled to a large storage tank in Norway. An analytical model was developed and validated with experimental data, and then it was used to optimise some parameters. Although the device performed well for clear and low humidity nights, the authors recommended analysing the performance of the system in climates with significant cooling demands, with outdoors nocturnal temperature not suitable to meet the comfort temperatures, to corroborate their simulation results.

Similarly to preceding research, Hosseinzadeh and Taherian (2012) [113] tested an unglazed radiator with storage in Iran. The experimental results were also used to validate an analytical model. The prototype showed an average net cooling power of 45 W/m^2 and capability of lowering 8°C a 130L water tank.

Also using a closed water-based system, Ferrer Tevar et al. (2015) [110] tested 3 different radiators with different infrared emissivities (0.02, 0.5 and 0.9) in Almeria, Spain. The one with

low emissivity material was used to isolate the effect of convection from the others. The experimental results showed averaged powers of $60\ W/m^2$. They conclude that the use of this technology could lower the cooling demands of buildings and also that is interesting to integrate it in buildings, specially combined with inertial elements.

Lately, Ahmadi et. al. (2016) [124] tested a prototype, using a plastic sheet as cover and with a storage tank, in Iran. The radiator surface reached temperatures 20°C below ambient temperature. It was also tested the influence of the numbers of plastic layers as cover showing that the best performance was achieved when there was a single layer.

Apart from research in testing specific devices, development and testing of new materials was also addressed. Bathgate and Bosi (2011) [86] used two different covers, Polyethylene (PE) and Zinc Sulphide (ZnS), to analyse its potential and to justify the use of ZnS instead of PE, based on the similar behaviour of both covers and the higher durability of ZnS. The study showed a good performance of both PE and ZnS covers, reaching 6°C below ambient and a total net heat radiation loss up to $580\ Wh/m^2night$ for PE and $470\ Wh/m^2night$ for ZnS.

Recent research have been conducted in order to find new ways to enhance radiative cooling or combine it with other technologies that could benefit its economical profit/overall performance [61,74,109,125].

Eicker and Dalibard (2011) [109] tested and developed a combination of radiative cooling with photovoltaic solar collector to produce cooling and electricity. This device was tested in Madrid, showing cooling powers of $60-65\ W/m^2$ when coupled to the heat sink storage tank (depending on the temperature the tank was used to cool a radiant floor or for heat rejection from a chiller), and $40-45\ W/m^2$ when directly used to cool down a ceiling containing phase change material (PCM). For this research, a numerical model was developed and validated.

Selective materials could improve the performance of radiative cooling in such a way that it can even work during daytime. Raman et al. (2014) [74] used the so called photonics design optimization to develop a material which can reflect 97% of the sunlight and also strongly emit in the infrared window. This improvement allows producing cooling during the whole day rather than only during the night. Empirical results showed a radiator temperature 5°C below ambient temperature and a $40\ W/m^2$ cooling power during exposition at direct sunlight conditions.

Finally, some research has been conducted in combining radiative cooling and solar heating [61,125,126] in the same device, showing a great potential. In [125] the systems was a vertical wall with a coated aluminium plate. This research showed perfect integration between the

building and the heating/cooling system. Further on this concept, Hu et. al. [61] developed and tested a selective material that performs well on both heating and cooling. Results showed a performance of 76.8% in heating and 75% in cooling compared to that of conventional systems. Afterwards, Hu et al. [126] used this material in a prototype whose performance was compared to a traditional flat-plate solar collector. In diurnal testing mode it showed a thermal efficiency of 86.4% compared to the traditional solar collector, whereas in cooling mode, it presented a cooling power density of $50 W/m^2$ when the radiator surface was at ambient temperature, as well as a capability of reaching 7.2°C below ambient temperature.

Research tendencies from the development of the first prototype have gone to the use of selective materials and the combination of radiative cooling with other technologies. The main goals are to reduce the payback time and to be able to provide different energy demands (e.g. cooling, heating, electricity).

6. Conclusions

In the present paper, research in the topic of radiative cooling is reviewed and classified, presenting the main results and conclusions. The articles are classified in four different sections: radiative cooling background, selective radiative cooling, theoretical approach and numerical simulation for radiative cooling, and radiative cooling prototypes.

Radiative cooling has been long, but not widely, analysed as a physical phenomenon in order to determine its influence in superficial heat balances, showing that, due to its low energy density, even minor heat fluxes are significant for the system performance. This phenomenon is fitted by straightforward correlations which are explained and summarized in the present work. These correlations depend on meteorological parameters, meaning that somehow they are very location dependant. As this phenomenon is not usually measured, the implementation potential for cooling purposes was barely analysed. Although correlations do not depict radiative cooling phenomenon better than real data, they can be used as a good approach, if adapted to the specific location. It is also important to mention that the radiation coming from the sky is not uniform through the spectrum as explained before; therefore the optical properties in the specific wave range (atmospheric window) may be important and should be accurately measured.

Given the low cooling power reached by this technology, different improvements have been analysed and studied. Materials with appropriate properties were fully analysed in the literature, from optical to thermal properties. General tendency leads to two possibilities: to develop/use materials that improve the cooling capacity of the system, or to develop/use materials that

provide other benefits to the system (such as solar collection, PV, structural strength, etc.). Currently the design of these materials has entered to a microscopically level of precision.

Despite radiative cooling is a novel technology, analytical approaches and numerical simulations are spread all over the literature. The research done is mainly orientated to flat plate design. This design presents similarities to a solar collector, since both designs have similar shape, both can adapt to the building envelope and both should face upward to the sky.

In the present review, the research about numerical simulations and prototypes has been classified bearing in mind the influencing parameters of the sky, the ambient, and the internal fluid. From this research, some interesting conclusions are extracted: (1) the use of cover is recommended to achieve low temperatures, (2) the use of water instead of air as a heat-carrier fluid is also recommended to control the system, and (3) heat storage is recommend to reach high cooling power densities.

Experimental analysis of this technology has also been widely performed in order to prove the concept and it has also been used to validate numerical models. Results show that the applicability of this technology is possible in some climates. These results lead new prototypes to provide new functionalities apart from radiative cooling for profitable reasons, such as generate heating using solar collection or electricity using PV.

Even though this is a low-grade technology and may not be enough for some particular requirements, the use of this technology for cooling purposes, actively or passively, can dramatically reduce the energy consumption, since it requires low energy for its operation and it comes from a renewable source.

Nevertheless, there exist some issues to be taken into account that limit the implementation of this technology. For instance, the use of a material with appropriate properties is an issue to be solved. Also, referring to simulations, some optical phenomena are omitted, when developing the model, related to electromagnetic optics or to photonics. This omission is a simplification of such complex effects. Finally, mention that this technology has a low energetic density for cooling purposes, so significant improvements are expected.

Thus, further research is warranted in order to determine the real potential of such technology, to develop new concepts and systems, and to overcome the main limitations existing at the moment.

Acknowledgements

Sergi Vall would like to thank the Secretaria d'Universitats i Recerca del Departament d'Economia i Coneixement de la Generalitat de Catalunya for his research fellowship.

Nomenclature

Symbol	Description	Equations where appears	Variable adapted
Δt	maximum day length (hour)	24	
$\Delta\varepsilon$	correction factor to take into account the day-night and seasonal variation (-)	24	
$\Delta\varepsilon_e$	pressure correction factor (-)	19, 20	
$\Delta\varepsilon_h$	diurnal correction factor (-)	17, 18, 19	$\Delta\varepsilon$ in [23]
A	factor that takes into account the variation of the emissivity	24	
clf	cloud fraction term (-) (see [38])	41	
C_p	specific heat of the fluid ($J \cdot kg^{-1} \cdot K^{-1}$) (see [115])	52	
e_0	partial pressure of water vapour (mbar).	4, 5, 6, 9, 10, 11, 12, 25, 26, 29, 30, 31, 32, 33, 40, 41, 42, 44, 45	e in [5,9–12,29,38,42,43], e_d in [39]
$\bar{e}_s^H$, $\bar{e}_{s,2}^H$ and η^H	parameters to compare radiative cooling selective materials (see [45]) (-)	49, 50, 51	
f	factor that takes into account the delay of the emissivity cycle in relation to the solar cycle (-)	24	
$f_{8,i}$	fraction of black body radiation emitted through the infrared window by layer "i" (-)	37	
F	collector efficiency factor (-)(see [115])	52	F' in [115]
H	relative humidity (%),	14	
$I_{b,\lambda}$	spectral radiance of a blackbody ($W \cdot m^{-3}$)	49, 50	W in [45]
k	empirical coefficient depending on the cloud type, to be defined in the original paper (-)	34	
$K(t)$,$L(t)$	correction factors (see values in [25])	23	$K(H), L(H)$ in [25]
K_0	daily clearness index (-) (see [37])	40	
$\dot{m}$	mass flow rate ($kg \cdot s^{-1}$) (see [115])	52	
n	number of parallel tubes (-)(see [115])	52	

P_0	atmospheric pressure (mbar)	20	P in [24]
R	effective outgoing infrared radiation from a surface on earth ($W \cdot m^{-2}$)	1, 34	I in [5], R_W in [33]
$R_{\uparrow}$	infrared radiation emitted by a surface on earth ($W \cdot m^{-2}$) normally calculated using Stefan-Boltzmann law	1	$I_{\uparrow}$ in [5]
$R_{\downarrow}$	infrared radiation from atmosphere, absorbed by a surface on earth ($W \cdot m^{-2}$).	1, 35, 37	R_T in [35], R_{ldc} in [36], LW_d in [38], $I_{\downarrow}$ in [5]
$R_{\downarrow,0}$	infrared radiation from atmosphere under clear sky conditions ($W \cdot m^{-2}$)	7, 35, 37, 45	$I_{\downarrow,0}$ in [5], E_a in [9,10,33],R in [11,14,15], R_A in [18], $F_{\downarrow}$ in [29], $F^{\downarrow}_{LW,clr}$ in [27], R_{LD} in [19], F in [31], R_a in [35], R_{ld} in [36], LW_{in} in [39]
R_0	effective outgoing infrared radiation under clear-sky conditions ($W \cdot m^{-2}$)	34, 43	R in [33]
s	ratio between the measured solar irradiance to the clear-sky irradiance (-)	41	
S	absorbed solar radiation per unit area ($W \cdot m^{-2}$) (see [115])	52	
$SCOP_{NET}$	estimated average seasonal performance factor of electrically driven heat pumps (-)		
t	time of the day (hour)	18	
t’	approximate hour of sunrise in solar time (hour)	24	
$[t(\lambda)/t_{av}]$ and b	empirical parameters (see [46]) (-)	48	
T_a	ambient dry bulb temperature (K).	3, 7, 8, 9, 10, 11, 12, 23, 30, 31, 32, 33, 40, 41, 42, 52	T in [5,11,14,15,31,38,39, 43], T_A in [18], T_0 in [19,20,27,29,30]
$T_{a,corrected}$	corrected ambient dry bulb temperature (K)	23	
$T_{c,i}$	cloud temperature of layer “i” (K)	37	T_i in [35]
T_{dp}	dew point temperature (ºC)	15, 16, 21, 22, 23, 27, 28	t_d in [25]
T_s	surface temperature (K)	49, 50	
T_f	temperature of the fluid at the desired point (normally the outlet fluid temperature) (K) (see [115])	52	

T_{fi}	inlet fluid temperature (K) (see [115])	52	
T_{sky}	effective sky temperature (K)	2, 40, 45	T_s in [37]
u, v	empirical parameters with different values depending on the different cloud types (-) (see [36])	39	
U_L	collector overall heat loss coefficient ($W \cdot m^{-2} \cdot K^{-1}$) (see [115])	52	
w	distance between parallel tubes (m) (see [115])	52	W in [115]
W	fractional area of sky covered by clouds (-)	34, 35, 36, 38, 39	A/A_i in [34,35], N in [22], n in [24], m_c in [36]
y	tubes length (m) (see [115])	52	
Z	altitude above sea level (km)	14	
$\alpha, \beta, \gamma, a, b$	empirical coefficients, to be defined in the original paper (-)	4, 5, 45	
γ	parameter to take into account humidity (see [42])	43, 44	
Γ	factor depending on the cloud base temperature (-) (see [24])	38	
ε_{sky}	effective sky emissivity (-)	3, 35, 36, 38, 39, 41, 42, 47, 48	ε in [22,24,38]
$\varepsilon_{sky,0}$	effective sky emissivity under clear sky conditions (-)	4, 5, 6, 7, 8, 9, 12, 14, 15, 16, 17, 19, 21, 22, 25, 26, 27, 28, 29, 30, 31, 32, 33, 35, 36, 38, 39, 48	ε_a in [7,20,29], $\varepsilon_0$in [22,24], ε_{sky} in [8,28], ε in [5,23,25], ε_{a0} in [19], ε_c in [38], e_a in [45],ε_s in [46]
$\varepsilon_{10.5-12.5,0}$ and $\varepsilon_{8-13,0}$	effective sky emissivity for the wavelength rage showed, under clear sky conditions (-)	10, 11	$\varepsilon_{10.5-12.5}$ and $\varepsilon_{8-13,0}$ in [20]
$\varepsilon_{cloud,i}$	emissivity of cloud layer "i" (-)	37	ε_i in [35], ε_c in [24]
$\varepsilon_{cloudy\ sky}$	equivalent sky emissivity with entirely cloudy sky	36	A in [22]
θ	zenith angle (rad)	43, 45, 46, 47, 48	z in [5,42,43]
λ	wavelength (μm)	46, 47, 48	
ξ	parameter to take into account humidity and ambient temperature (see [30]) ($g \cdot cm^{-2}$)	31	
σ	Stefan-Boltzmann's constant: $5.6704 \cdot 10^{-8} (W \cdot m^{-2} \cdot K^{-4})$	2, 3, 33, 37, 45	
ρ	reflectivity (-)	49, 50	R in [45]
τ	parameter to take into account humidity and ambient temperature	32	

	(see [31])		
τ_8	transmittance of the atmosphere in the infrared window (-)	37	

References

[1] European Parliament. Directive 2010/31/EU of the European Parliament and of the Council of 19 May 2010 on the energy performance of buildings. Off J Eur Union 2010;153:13–35.

[2] European Parliament. Directive 2009/28/EC of the European Parliament and of the Council of 23 April 2009 on the promotion of the use of energy from renewable sources and amending and subsequently repealing Directives 2001/77/EC and 2003/30/EC. Off J Eur Union 2009;140:16–62. doi:10.3000/17252555.L_2009.140.eng.

[3] European Commission. Decision of 1 March 2013 (2013/114/EU) establishing the guidelines for Member States on calculating renewable energy from heat pumps from different heat pump technologies pursuant to Article 5 of Directive 2009/28/EC of the European Parliament and of the . Off J Eur Union 2013;62:27–35.

[4] Lu X, Xu P, Wang H, Yang T, Hou J. Cooling potential and applications prospects of passive radiative cooling in buildings: The current state-of-the-art. Renew Sustain Energy Rev 2016;65:1079–97. doi:10.1016/j.rser.2016.07.058.

[5] Sellers WD. Physical Climatology. Chicago & London: University of Chicago; 1965.

[6] Bell E, Eisner L, Young J, Oetjen R. Spectral-Radiance of Sky and Terrain at Wavelengths between 1 and 20 Microns. II. Sky Measurements. J Opt Soc Am 1960;50:1313–20. doi:10.1364/JOSA.50.001313.

[7] Bliss RW. Atmospheric radiation near the surface of the ground: A summary for engineers. Sol Energy 1961;5:103–20. doi:10.1016/0038-092X(61)90053-6.

[8] Berdahl P, Fromberg R. The thermal radiance of clear skies. Sol Energy 1982;29:299–314. doi:10.1016/0038-092X(82)90245-6.

[9] Ångström AK. A study of the radiation of the atmosphere. Smithson Inst Misc Collect 1915;65:159.

[10] Ångström AK. Effective radiation during the second international polar year. Medde Stat Met Hydrogr Anst 1936;6.

[11] Brunt D. Notes on radiation in the atmosphere. I. Q J R Meteorol Soc 1932;58:389–420. doi:10.1002/qj.49705824704.

[12] Elsasser WM. Heat transfer by infrared radiation in the atmosphere. Harvard University Press; 1942.

[13] Kondratyev KY. Radiation in the Atmosphere. New York: Academic Press; 1969.

[14] Swinbank WC. Long-wave radiation from clear skies. Q J R Meteorol Soc 1963;89:339–48. doi:DOI: 10.1002/qj.49708938105.

[15] Idso SB, Jackson RD. Thermal radiation from the atmosphere. J Geophys Res 1969;74:5397–403.

[16] Aase JK, Idso SB. A comparison of two formula types for calculating long-wave radiation from the atmosphere. Water Resour Res 1978;14:623–5. doi:10.1029/WR014i004p00623.

[17] Hatfield JL, Reginato RJ, Idso SB. Comparison of long-wave radiation calculation methods over the United States. Water Resour Res 1983;19:285.

doi:10.1029/WR019i001p00285.

[18] Satterlund DR. An improved equation for estimating long-wave radiation from the atmosphere. Water Resour Res 1979;15:1649. doi:10.1029/WR015i006p01649.

[19] Brutsaert W. On a Derivable Formula for Long-Wave Radiation From Clear Skies. Water Resour Res 1975;11:742–4. doi:10.1029/WR011i005p00742.

[20] Idso SB. A Set of Equations for Full Spectrum and 8- to 14 micron and 10.5- to 12.5 micron Thermal Radiation From Cloudless Skies. Water Resour Res 1981;17:295–304. doi:10.1029/WR017i002p00295.

[21] Andreas EL, Ackley SF. On the Differences in Ablation Seasons of Arctic and Antarctic Sea Ice. J Atmos Sci 1982;39:440–7. doi:10.1175/1520-0469(1982)039<0440:OTDIAS>2.0.CO;2.

[22] Centeno V M. New formulae for the equivalent night sky emissivity. Sol Energy 1982;28:489–98. doi:10.1016/0038-092X(82)90320-6.

[23] Berdahl P, Martin M. Emissivity of clear skies. Sol Energy 1984;32:663–4. doi:10.1016/0038-092X(84)90144-0.

[24] Martin M, Berdahl P. Characteristics of infrared sky radiation in the United States. Sol Energy 1984;33:321–36. doi:10.1016/0038-092X(84)90162-2.

[25] Berger X, Buriot D, Garnier F. About the equivalent radiative temperature for clear skies. Sol Energy 1984;32:725–33. doi:10.1016/0038-092X(84)90247-0.

[26] Alados-Arboledas L, Jimenez JI. Day-night differences in the effective emissivity from clear skies. Boundary-Layer Meteorol 1988;45:93–101. doi:10.1007/BF00120817.

[27] Niemelä S, Räisänen P, Savijärvi H. Comparison of surface radiative flux parameterizations part I: Longwave radiation. Atmos Res 2001;58:1–18. doi:10.1016/S0169-8095(01)00084-9.

[28] Tang R, Etzion Y, Meir IA. Estimates of clear night sky emissivity in the Negev Highlands, Israel. Energy Convers Manag 2004;45:1831–43. doi:10.1016/j.enconman.2003.09.033.

[29] Staley DO, Jurica GM. Effective Atmospheric Emissivity under Clear Skies. J Appl Meteorol Climatol 1972;11:349–56. doi:10.1175/1520-0450(1972)011<0349:EAEUCS>2.0.CO;2.

[30] Prata AJ. A new long-wave formula for estimating downward clear-sky radiation at the surface. Q J R Meteorol Soc 1996;122:1127–51.

[31] Dilley AC, O'Brien DM. Estimating downward clear sky long-wave irradiance at the surface from screen temperature and precipitable water. Q J R Meteorol Soc 1998;124:1391–401.

[32] Viúdez-Mora A, Calbó J, González JA, Jiménez MA. Modeling atmospheric longwave radiation at the surface under cloudless skies. J Geophys Res Atmos 2009;114:1–12. doi:10.1029/2009JD011885.

[33] Ångström AK. Radiation and the Temperature of snow and convection of the air at its surface. Akt För Mat Astron Och Fys 1919;13:1–18.

[34] Bolz HM. Die Abhängigkeit der infraroten Gegenstrahlung von der Bewölkung. Meteorol Zeitschrift 1949;3:201–3.

[35] Kimball B a., Idso SB, Aase JK. A model of thermal radiation from partly cloudy and overcast skies. Water Resour Res 1982;18:931. doi:10.1029/WR018i004p00931.

[36] Sugita M, Brutsaert W. Cloud effect in the estimation of instantaneous downward longwave radiation. Water Resour Res 1993;29:599–605. doi:10.1029/92WR02352.

[37] Aubinet M. Longwave sky radiation parametrizations. Sol Energy 1994;53:147–54.

doi:10.1016/0038-092X(94)90475-8.

[38] Crawford TM, Duchon CE. An Improved Parameterization for Estimating Effective Atmospheric Emissivity for Use in Calculating Daytime Downwelling Longwave Radiation. J Appl Meteorol 1999;38:474–80. doi:10.1175/1520-0450(1999)038<0474:AIPFEE>2.0.CO;2.

[39] Sridhar V, Elliott RL. On the development of a simple downwelling longwave radiation scheme. Agric For Meteorol 2002;112:237–43. doi:10.1016/S0168-1923(02)00129-6.

[40] Viúdez-Mora A, Costa-Surós M, Calbó J, González JA. Journal of Geophysical Research : Atmospheres. J Geophys Res Atmos 2014;120:199–214. doi:10.1002/2014JD022310.Received.

[41] Malek E. Evaluation of effective atmospheric emissivity and parameterization of cloud at local scale. Atmos Res 1997;45:41–54. doi:10.1016/S0169-8095(97)00020-3.

[42] Linke F. Die Nächtliche effektive Ausstrahlung unter verschiedenen Zenitdistanzen. Meteorol Zeitschrift 1931;48:25–31.

[43] Strong J. Study of Atmospheric Absorption and Emission in the Infrared Spectrum. J Franklin Inst 1941;232:22.

[44] Cook J. Radiative cooling. Passiv. Cool., Cambridge and London: MIT Press; 2000, p. 606.

[45] Granqvist CG, Hjortsberg A. Radiative cooling to low temperatures: General considerations and application to selectively emitting SiO films. J Appl Phys 1981;52:4205–20. doi:10.1063/1.329270.

[46] Martin M, Berdahl P. Summary of results from the spectral and angular sky radiation measurement program. Sol Energy 1984;33:241–52. doi:10.1016/0038-092X(84)90155-5.

[47] Atwater MA, Ball JT. Computation of IR sky temperature and comparison with surface temperature. Sol Energy 1978;21:211–6. doi:10.1016/0038-092X(78)90023-3.

[48] Exell RHB. The atmospheric radiation climate of Thailand. Sol Energy 1978;21:73–9. doi:10.1016/0038-092X(78)90032-4.

[49] Hanif M, Mahlia TMI, Zare a., Saksahdan TJ, Metselaar HSC. Potential energy savings by radiative cooling system for a building in tropical climate. Renew Sustain Energy Rev 2014;32:642–50. doi:10.1016/j.rser.2014.01.053.

[50] Pissimanis DK, Notaridou V a. The atmospheric radiation in Athens during the summer. Sol Energy 1981;26:525–8. doi:10.1016/0038-092X(81)90164-X.

[51] Argiriou A, Santamouris M, Assimakopoulos DN. Assessment of the radiative cooling potential of a collector using hourly weather data. Energy 1994;19:879–88. doi:10.1016/0360-5442(94)90040-X.

[52] Burch J, Christensen C, Salasovich J, Thornton J. Simulation of an unglazed collector system for domestic hot water and space heating and cooling. Sol Energy 2004;77:399–406. doi:10.1016/j.solener.2003.12.014.

[53] Catalanotti S, Cuomo V, Piro G, Ruggi D, Silvestrini V, Troise G. The radiative cooling of selective surfaces. Sol Energy 1975;17:83–9. doi:10.1016/0038-092X(75)90062-6.

[54] Bartoli B, Catalanotti S, Coluzzi B, Cuomo V, Silvestrini V, Troise G. Nocturnal and diurnal performances of selective radiators. Appl Energy 1977;3:267–86. doi:10.1016/0306-2619(77)90015-0.

[55] Addeo A, Monza E, Peraldo M, Bartoli B, Coluzzi B, Silvestrini V, et al. Selective covers for natural cooling devices. Nuovo Cim C 1978;1:419–29. doi:10.1007/BF02507668.

[56] Granqvist CG. Radiative heating and cooling with spectrally selective surfaces. Appl Opt 1981;20:2606–15.

[57] Granqvist CG, Hjortsberg A, Eriksson TS. Radiative Cooling to Low Temperatures with Selectively IR-Emitting Surfaces. Thin Solid Films 1982;90:187–90.

[58] Trombe F. Perspectives sur l'utilisation des rayonnements solaires et terrestres dans certaines régions du monde. Rev Générale Therm 1967;6:1285–314.

[59] Grenier P. Réfrigération radiative. Effet de serre inverse. Rev Phys Appliquée 1979;14:87–90. doi:10.1051/rphysap:0197900140108700.

[60] Matsuta M, Terada S, Ito H. Solar Heating and radiative cooling using a solar collector-sky radiator with a spectrally selective surface. Sol Energy 1987;39:183–6.

[61] Hu M, Pei G, Li L, Zheng R, Li J, Ji J. Theoretical and Experimental Study of Spectral Selectivity Surface for Both Solar Heating and Radiative Cooling. Int J Photoenergy 2015;2015:1–9. doi:10.1155/2015/807875.

[62] Hjortsberg A, Granqvist CG. Infrared optical properties of silicon monoxide films. Appl Opt 1980;19:1694–6.

[63] Eriksson TS, Granqvist CG. Infrared optical properties of electron-beam evaporated silicon oxynitride films. Appl Opt 1983;22:3204–6.

[64] Eriksson TS, Lushiku EM, Granqvist CG. Materials for radiative cooling to low temperature. Sol Energy Mater 1984;11:149–61.

[65] Eriksson TS, Jiang S-J, Granqvist CG. Surface coatings for radiative cooling applications: silicon dioxide and silicon nitride made by reactive RF-sputtering. Sol Energy Mater 1985;12:319–25.

[66] Diatezua MD, Thiry PA, Caudano R. Characterization of silicon oxynitride multilayered systems for passive radiative cooling application. Vacuum 1995;46:1121–4. doi:10.1016/0042-207X(95)00120-4.

[67] Tazawa M, Jin P, Tanemura S. Thin film used to obtain a constant temperature lower than the ambient. Thin Solid Films 1996;281–282:232–4. doi:10.1016/0040-6090(96)08620-8.

[68] Tazawa M, Jin P, Yoshimura K, Miki T, Tanemura S. New material design with V1−xWxO2 film for sky radiator to obtain temperature stability. Sol Energy 1998;64:3–7. doi:10.1016/S0038-092X(98)00057-7.

[69] Berdahl P. Radiative cooling with MgO and/or LiF layers. Appl Opt 1984;23:370. doi:10.1364/AO.23.000370.

[70] Harrison AW, Walton MR. Radiative cooling of TiO2 white paint. Sol Energy 1978;20:185–8.

[71] Awanou CN. Radiative Cooling by a Diode Roof. Sol Wind Technol 1986;3:163–72. doi:10.1016/0741-983X(86)90030-5.

[72] Orel B, Klanjsek Gunde M, Krainer A. Radiative Cooling Efficiency of White Pigmented Paints. Sol Energy 1993;50:477–82.

[73] Rephaeli E, Raman A, Fan S. Ultrabroadband Photonic Structures To Achieve High-Performance Daytime Radiative Cooling. Nano Lett 2013;13:A-E. doi:10.1021/nl4004283.

[74] Raman AP, Anoma MA, Zhu L, Rephaeli E, Fan S. Passive radiative cooling below ambient air temperature under direct sunlight. Nature 2014;515:540–4. doi:10.1038/nature13883.

[75] Nilsson NA, Eriksson TS, Granqvist CG. Infrared-transparent convection shields for radiative cooling: Initial results on corrugated polyethylene foils. Sol Energy Mater

1985;12:327–33. doi:10.1016/0165-1633(85)90002-4.

[76] Ali AHH, Saito H, Taha IMS, Kishinami K, Ismail IM. Effect of aging, thickness and color on both the radiative properties of polyethylene films and performance of the nocturnal cooling unit. Energy Convers Manag 1998;39:87–93. doi:10.1016/S0196-8904(96)00174-4.

[77] Gentle AR, Dybdal KL, Smith GB. Polymeric mesh for durable infra-red transparent convection shields: Applications in cool roofs and sky cooling. Sol Energy Mater Sol Cells 2013;115:79–85. doi:10.1016/j.solmat.2013.03.001.

[78] Nilsson TMJ, Niklasson GA, Granqvist CG. A solar reflecting material for radiative cooling applications: ZnS pigmented polyethylene. Sol Energy Mater Sol Cells 1992;28:175–93. doi:10.1016/0927-0248(92)90010-M.

[79] Nilsson TMJ, Niklasson GA. Radiative cooling during the day: simulations and experiments on pigmented polyethylene cover foils. Sol Energy Mater Sol Cells 1995;37:93–118. doi:10.1016/0927-0248(94)00200-2.

[80] Mastai Y, Diamant Y, Aruna ST, Zaban A. TiO2 Nanocrystalline Pigmented Polyethylene Foils for Radiative Cooling Applications: Synthesis and Characterization. Langmuir 2001;17:7118–23.

[81] Engelhard T, Jones ED, Viney I, Mastai Y, Hodes G. Deposition of tellurium ® lms by decomposition of electrochemically- generated H 2 Te : application to radiative cooling devices 2000;370:101–5.

[82] Dobson KD, Hodes G, Mastai Y. Thin semiconductor films for radiative cooling applications. Sol Energy Mater Sol Cells 2003;80:283–96. doi:10.1016/j.solmat.2003.06.007.

[83] Benlattar M, Oualim EM, Harmouchi M, Mouhsen A, Belafhal A. Radiative properties of cadmium telluride thin film as radiative cooling materials. Opt Commun 2005;256:10–5. doi:10.1016/j.optcom.2005.06.033.

[84] Benlattar M, Oualim EM, Mouhib T, Harmouchi M, Mouhsen A, Belafhal A. Thin cadmium sulphide film for radiative cooling application. Opt Commun 2006;267:65–8. doi:10.1016/j.optcom.2006.06.050.

[85] Mouhib T, Mouhsen A, Oualim EM, Harmouchi M, Vigneron JP, Defrance P. Stainless steel/tin/glass coating as spectrally selective material for passive radiative cooling applications. Opt Mater (Amst) 2009;31:673–7. doi:10.1016/j.optmat.2008.07.010.

[86] Bathgate SN, Bosi SG. A robust convection cover material for selective radiative cooling applications. Sol Energy Mater Sol Cells 2011;95:2778–85. doi:10.1016/j.solmat.2011.05.027.

[87] Hjortsberg A, Granqvist CG. Radiative cooling with selectively emitting ethylene gas. Appl Phys Lett 1981;39:507–9. doi:10.1063/1.92783.

[88] Lushiku EM, Eriksson TS, Hjortsberg A, Granqvist CG. Radiative cooling to low temperatures with selectively infrared-emitting gases. Sol Wind Technol 1984;1:115–21. doi:10.1016/0741-983X(84)90013-4.

[89] Lushiku EM, Granqvist CG. Radiative cooling with selectively infrared-emitting gases. Appl Opt 1984;23:1835–43. doi:10.1364/AO.23.001835.

[90] Lushiku EM, Granqvist CG. Radiative cooling with selectively infrared-emitting ammonia gase. J Appl Phys 1982;53:5526–30. doi:10.1364/AO.23.001835.

[91] Du Marchie Van Voorthuysen E, Roes R. Blue sky cooling for parabolic trough plants. Energy Procedia 2013;49:71–9. doi:10.1016/j.egypro.2014.03.008.

[92] Hull JR, Schertz WW. Evacuated-tube directional-radiating cooling system. Sol Energy 1985;35:429–34. doi:10.1016/0038-092X(85)90132-X.

[93] Smith GB. Amplified radiative cooling via optimised combinations of aperture geometry and spectral emittance profiles of surfaces and the atmosphere. Sol Energy Mater Sol Cells 2009;93:1696–701. doi:10.1016/j.solmat.2009.05.015.

[94] Johnson TE. Radiation cooling of structures with infrared transparent wind screens. Sol Energy 1975;17:173–8. doi:10.1016/0038-092X(75)90056-0.

[95] Landro B, McCormick PG. Effect of surface characteristics and atmospheric conditions on radiative heat loss to a clear sky. Int J Heat Mass Transf 1980;23:613–20. doi:10.1016/0017-9310(80)90004-6.

[96] Berdahl P, Martin M, Sakkal F. Thermal Performance of Radiative Cooling Panels. Int J Heat Mass Transf 1983;26:871–80. doi:10.1016/S0017-9310(83)80111-2.

[97] Hamza H. Ali A, Taha IMS, Ismail IM. Cooling of water flowing through a night sky radiator. Sol Energy 1995;55:235–53. doi:10.1016/0038-092X(95)00030-U.

[98] Al-Nimr M., Kodah Z, Nassar B. A theoretical and experimental investigation of a radiative cooling system. Sol Energy 1998;63:367–73. doi:10.1016/S0038-092X(98)00098-X.

[99] Al-Nimr M, Tahat M, Al-Rashdan M. A night cold storage system enhanced by radiative cooling—a modified Australian cooling system. Appl Therm Eng 1999;19:1013–26. doi:10.1016/S1359-4311(98)00103-3.

[100] Mihalakakou G, Ferrante A, Lewis JO. The cooling potential of a metallic nocturnal radiator. Energy Build 1998;28:251–6. doi:10.1016/S0378-7788(98)00006-1.

[101] Farmahini Farahani M, Heidarinejad G, Delfani S. A two-stage system of nocturnal radiative and indirect evaporative cooling for conditions in Tehran. Energy Build 2010;42:2131–8. doi:10.1016/j.enbuild.2010.07.003.

[102] Heidarinejad G, Farmahini Farahani M, Delfani S. Investigation of a hybrid system of nocturnal radiative cooling and direct evaporative cooling. Build Environ 2010;45:1521–8. doi:10.1016/j.buildenv.2010.01.003.

[103] Farmahini-Farahani M, Heidarinejad G. Increasing effectiveness of evaporative cooling by pre-cooling using nocturnally stored water. Appl Therm Eng 2012;38:117–23. doi:10.1016/j.applthermaleng.2012.01.023.

[104] Zhang S, Niu J. Cooling performance of nocturnal radiative cooling combined with microencapsulated phase change material (MPCM) slurry storage. Energy Build 2012;54:122–30. doi:10.1016/j.enbuild.2012.07.041.

[105] Sima J, Sikula O, Kosutova K, Plasek J. Theoretical Evaluation of Night Sky Cooling in the Czech Republic. Energy Procedia 2014;48:645–53. doi:10.1016/j.egypro.2014.02.075.

[106] Erell E, Etzion Y. Analysis and Experimental Verification of an Improved Cooling Radiator. Renew Energy 1999;16:700–3.

[107] Erell E, Etzion Y. Radiative cooling of buildings with flat-plate solar collectors. Build Environ 2000;35:297–305. doi:10.1016/S0360-1323(99)00019-0.

[108] Bagiorgas HS, Mihalakakou G. Experimental and theoretical investigation of a nocturnal radiator for space cooling. Renew Energy 2008;33:1220–7. doi:10.1016/j.renene.2007.04.015.

[109] Eicker U, Dalibard A. Photovoltaic-thermal collectors for night radiative cooling of buildings. Sol Energy 2011;85:1322–35. doi:10.1016/j.solener.2011.03.015.

[110] Ferrer Tevar JA, Castaño S, Garrido Marijuán A, Heras MR, Pistono J. Modelling and experimental analysis of three radioconvective panels for night cooling. Energy Build 2015;107:37–48. doi:10.1016/j.enbuild.2015.07.027.

[111] Sameti M, Kasaeian A. Numerical simulation of combined solar passive heating and

radiative cooling for a building. Build Simul 2015;8:239–53. doi:10.1007/s12273-015-0215-x.

[112] Man Y, Yang H, Qu Y, Fang Z. A Novel Nocturnal Cooling Radiator Used for Supplemental Heat Sink of Active Cooling System. Procedia Eng 2015;121:300–8. doi:10.1016/j.proeng.2015.08.1072.

[113] Hosseinzadeh E, Taherian H. An Experimental and Analytical Study of a Radiative Cooling System with Unglazed Flat Plate Collectors. Int J Green Energy 2012;9:766–79. doi:10.1080/15435075.2011.641189.

[114] Etzion Y, Erell E. Low-Cost Long-Wave Radiators for Passive Cooling of Buildings. Archit Sci Rev 1999;42:79–85. doi:10.1080/00038628.1999.9696856.

[115] Duffie JA, Beckman WA. Solar Engineering of Thermal Processes. Hoboken, NJ, USA: John Wiley & Sons, Inc.; 2013. doi:10.1002/9781118671603.

[116] Meir MG, Rekstad JB, LØvvik OM. A study of a polymer-based radiative cooling system. Sol Energy 2002;73:403–17. doi:10.1016/S0038-092X(03)00019-7.

[117] Michell D, Biggs KL. Radiation cooling of buildings at night. Appl Energy 1979;5:263–75.

[118] Dan PD, Chinnappa JCV. The cooling of water flowing over an inclined surface exposed to the night sky. Sol Wind Technol 1989;6:41–50. doi:10.1016/0741-983X(89)90036-2.

[119] Ezekwe CI. Performance of a heat pipe assisted night sky radiative cooler. Energy Convers Manag 1990;30:403–8. doi:10.1016/0196-8904(90)90041-V.

[120] Ito S, Miura N. Studies of Radiative Cooling Systems for Storing Thermal Energy. J Sol Energy Eng 1989;111:251–6. doi:10.1115/1.3268315.

[121] Etzion Y, Erell E. Thermal storage mass in radiative cooling systems. Build Environ 1991;26:389–94. doi:10.1016/0360-1323(91)90065-J.

[122] Erell E, Etzion Y. A Radiative Cooling System Using Water as a Heat Exchange Medium. Archit Sci Rev 1992;35:39–49. doi:10.1080/00038628.1992.9696712.

[123] Erell E, Etzion Y. Heating experiments with a radiative cooling system. Build Environ 1996;31:509–17. doi:10.1016/0360-1323(96)00030-3.

[124] Ahmadi A, Karaei MA, Fallah H. Investigation of Night (Radiative) Cooling Event and Construction of Experimental Radiator. Int J Adv Biotechnol Res 2016;7:1180–4.

[125] Yong C, Yiping W, Li Z. Performance analysis on a building-integrated solar heating and cooling panel. Renew Energy 2015;74:627–32. doi:10.1016/j.renene.2014.08.076.

[126] Hu M, Pei G, Wang Q, Li J, Wang Y, Ji J. Field test and preliminary analysis of a combined diurnal solar heating and nocturnal radiative cooling system. Appl Energy 2016;179:899–908. doi:10.1016/j.apenergy.2016.07.066.